The Pennsylvania State University

The Graduate School

Department of Energy and Mineral Engineering

CARBON DIOXIDE SEQUESTRATION IN COAL: CHARACTERIZATION OF MATRIX DEFORMATION, SORPTION CAPACITY AND DYNAMIC PERMEABILITY AT IN-SITU STRESS CONDITIONS

A Dissertation in

Energy and Geo-Environmental Engineering

by

Jean Denis Nda'si Pone

Submitted in Partial Fulfillment
of the Requirements
for the Degree of

Doctor of Philosophy

May 2009

The dissertation of Jean Denis N. Pone was reviewed and approved* by the following:

Jonathan P. Mathews
Assistant professor, Energy and Mineral Engineering
Dissertation Advisor
Chair of Committee

Phillip M. Halleck
Associate Professor, Energy and Geo-Environmental Engineering

Derek Elsworth
Professor, Energy and Geo-Environmental Engineering

Demian Saffer
Associate Professor of Geosciences

Yaw D. Yeboah
Professor, Energy and Geo-Environmental Engineering
Head of the Department of Energy and Mineral Engineering

*Signatures are on file in the Graduate School

ABSTRACT

Sequestration of anthropogenic carbon dioxide in geological formation is one of the climate change mitigation options. The successful application of this technology is dependent on reliable estimates of carbon dioxide storage capacity and insightful indication of the variability of geological storage. Injection into deep, unmineable coal formations is one option being investigated. Current basic CO_2 sequestration work on powdered coal does not adequately capture the science of gas flow and storage processes at geologic sequestration conditions. To better assess the storage capacity and flow properties of CO_2 and CH_4 in coal, it is important to characterize the interplay of the various physical and chemical processes occurring during gas injection or production at simulated confining stress conditions representative of sequestration depths. In this thesis, the interactions of CO_2 and CH_4 with powder, non-powder unconfined, and non-powder confined bituminous coal were investigated under different stress conditions. The effects of stress on coal behavior at simulated sequestration conditions were determined. It includes the characterization of three-dimensional regional strain distribution induced by the application of stress, the sorption and desorption of CO_2 determined with X-ray computer tomography. Carbon dioxide and methane sorption capacity was evaluated using the volumetric method. Dynamic permeability of coal under different stress condition was determined using a transient-pulse approach. Results demonstrated that the deformations of a dry bituminous coal core upon stress application, or by CO_2 sorption or desorption are highly heterogeneous and differ among the various lithotype bands of a bituminous coal. Coal swelling was observed, but the extent was attenuated by

compression/compaction in adjacent lithotype bands. The CO_2 and CH_4 sorption capacity and sorption rates are reduced under stress, emphasizing that estimates of storage capacity and transport parameters based on powdered unconfined coal samples are misleading for sequestration capacity predictions. The application of 6.9 and 13.8 MPa of confining stress contributed to 39% and 64% of CO_2 sorption capacity reductions respectively in comparison to powder coal. Similarly, 85% and 91% CH_4 uptake capacity reductions due to 6.9 and 13.8 MPa of confining stress in comparison to powder coal were recorded. Due to presumed methane's limited ability to dissolve in coal matrix compared to CO_2, its sorption capacity reduction with applied stress was more pronounced. Coal permeability decreases with increasing confining stress. Average permeability was 0.001865 millidarcies when subjected to 6.9 MPa and decrease around 4 times to 0.000427 millidarcies when the confining stress was doubled. This decrease is likely due to the cleat and pore aperture reduction with increasing effective stress. Coal permeability also decreases over time even at constant effective stress. Permeability for both confining stress values decrease over time although at different rate: 26% reduction at 6.9 MPa and 47 % at 13.8 MPa. This reduction can likely be attributed to the swelling, structure rearrangement or compression/compaction of certain lithotypes occurring at different time-scales when exposed to CO_2.

TABLE OF CONTENTS

LIST OF FIGURES

LIST OF TABLES

ACKNOWLEDGEMENTS

I had the privilege of conducting graduate research on coal with someone who understands it thoroughly: Dr. Jonathan Mathews. He is patient, understanding, accessible, and knowledgeable. He has been a great advisor, mentor and friend to me throughout my research, and I thank him for that.

I am grateful to my committee members: Dr. Phil Halleck, Dr. Derek Elsworth and Dr. Demian Saffer. Each of them generously gave their time and assistance to make this a viable research and, undoubtedly, better than anything I could have completed alone. I will always be indebted to them for the training and skills they provided me over the course of my time at Penn State.

This project would not have been possible without Dr. Timothy Ryan assistance in teaching me how to analyses CT images. I wholly appreciate all of his help. Thank you to Dr. Abraham Grader for his assistance and suggestions at the beginning of this project. Thank you to Sultan El Enezi for his help during my data collection.

Finally and most importantly, I want to thank my family. My parents and my siblings have been supportive of my education throughout my life, and graduate school was no exception. Leaving industry for graduate school required a fairly significant lifestyle adjustment – one that my wife Sidonie was graciously willing to make. Her love, support and encouragement has been constant on this journey, and I thank her for that. Our son, Bill, was born while I was in graduate school, and he probably has no idea that his future was the reason I decided to return for a Ph.D.

Chapter 1

Introduction

Geological sequestration of CO_2 is one approach to mitigate climate change. The Intergovernmental Panel on Climate Change (IPCC) sees carbon capture and storage as offering great potential: in various scenarios it may account for between 15 and 55% of anthropogenic greenhouse gases reduction by 2100 (IPCC, 2005). Information and experience gained from the injection and/or storage of CO_2 from large number of existing enhanced oil recovery projects, as well as from the Sleipner, Weyburn and In-Salah projects, indicate that it is feasible to store CO_2 in geological formations as a CO_2 mitigation option. While there are uncertainties, the global geological CO_2 storage capacity is large. Deep coal seams that are not economically viable for coal production are one of the mitigation options investigated (Shi and Durucan, 2005). However, CO_2 storage capacity in unmineable coal formation is uncertain, with worldwide estimates ranging from as little as 3 $GtCO_2$ up to 200 $GtCO_2$. An added benefit of sequestering CO_2 in coal is the recovery of methane (Brown et al., 2007; Busch et al., 2004). However, carbon dioxide storage in coal, in conjunction with enhanced coalbed methane technology, is not well developed and a better characterization and quantification of coal matrix deformation, sorption capacity and flow processes in coals at geologic conditions of stress is needed. The injection and recovering of gas from coal is complicated by the interplay of competing processes and coal heterogeneity. Coal is a mixture of optically, chemically, and physically different structures (Stopes, 1919; Tideswell and Wheeler,

1919). The presences of visually obvious bands (lithotypes) composed of different macerals, derived from different parts of coal precursors are good indication of coal complexity. Two comprehensive reviews by White et al. (2005) and Halloway (2005) compiled some of the scientific and technological challenges impeding the effective deployment of carbon sequestration in coal.

The interaction of polar molecules with coal has been investigated over the years and has produced a large amount of pertinent data for sorption in coal (Kini et al., 1956; Levine, 1982; Nandi et al., 1956). A comprehensive summary of these discussions was presented by Anderson et al. (1956) and it was concluded that the sorption of polar molecules is complicated by swelling and imbibitions. Carbon dioxide interacts with different lithotype layers, and penetrates into macerals, to different extents and rates (Brenner, 1983). These lithotype bands and macerals also swell to different extents (Brenner, 1983; Brenner, 1985; Karacan, 2003). Walker et al.(1988) attributes CO_2 induced coal swelling (particles in a dilatometer with some stress) at high gas pressures to an equal combination of sorption in the pores and imbibed CO_2 into the coal structure. They also suggested that additional swelling should be expected if the stress was reduced. However, they did not speculate if this increased swelling would further increase capacity for CO_2. The expectation is that overburden stress will constrain swelling and, by inference, will decrease sorption capacity. Experiments performed on pulverized coal do not utilize confining stress, and thus do not represent the sequestration conditions. The swelling, which is anisotropic, reduces coal seam permeability by changing flow pathways dimensions, particularly the aperture, or width of cleats, micro-cleats and pores.

A direct consequence of the coal structure changes is the loss of injectivity during field operations (Mazumder et al., 2006). Moisture and methane removal causes shrinkage of the coal matrix. Increased pore pressure during gas injection however, leads to decreased effective stress and a competing deformation processes occur. These competing processes influence permeability (Harpalani and Chen, 1997) and are complicated by the lithotype specific kinetics of sorption/desorption, which are much slower in whole coals in comparison to pulverized coal. Confining stress is expected to influence cleat aperture and thus reduce cleat capacity. The impact of confining stress on sorption capacity is more severe for methane due to its inability to dissolve into coal matrix compare to CO_2. The application of confining stress reduces capacity by impacting coal's pore space and its ability to swell.

The amount of CO_2 that can be sequestered by a coal seam depends on its thickness, cleats distribution, maceral composition, mineral content, moisture content, stress, temperature, maturation extent and resultant behavior of the coal. *The hypothesis of this thesis is that the extent of deformation determines the dynamic permeability and hence the transport of gas in coal, influencing both the rate and capacity of the coalbed to accommodate CO_2 storage and provide methane production*. Swelling is governed by relaxation of the coal structure. Thus if the swelling ability is hindered, the sorption capacity is likely impacted. The CO_2 capacity is a combination of the capacities within macroporosity, mesoporosity, microporosity, and the swelling induced-capacity. Few experiments have evaluated whole-coal samples under in-situ stress conditions with an assessment of the sorption capacity, the uptake rate and the permeability evolution in time. The objectives of this thesis are:

1. The 3D characterization of coal regional strain behavior during compression, CO_2 uptake, and desorption of a bituminous coal at simulated in-situ stress conditions. (Chapter 2).
2. The characterization of the sorption rates and sorption capacities of carbon dioxide, methane in a bituminous coal sample under in-situ stress conditions. (Chapter 3).
3. Evaluate the dynamic permeability of a bituminous coal under in-situ stress conditions (Chapter 4).

The goal of this work is to elucidate the influence of confining stress on these three components (deformation, sorption capacity and permeability) and also further investigate the extent of the conflicting swelling/shrinking processes that occurs in CO_2 sequestration in coal.

This thesis comprises a series of papers either published or submitted for conferences or journal publication. In chronological order these papers are:

1. Pone, J.D.N., Halleck, P.M., Mathews, J.P., 2008. Detailed 3D characterization of coal strains induced by compression, carbon dioxide sorption, and desorption at simulated in-situ conditions. Asia Pacific Coalbed Methane Symposium, 22-24 September, Brisbane, Australia.
2. Pone, J.D.N., Hile, M., Halleck, P.M., Mathews, J.P., 2009. Three-dimensional carbon dioxide-induced strain distribution within a confined bituminous coal, International Journal of Coal Geology, 77(1-2)103-108.

3. Pone, J.D.N., Halleck, P.M., Mathews, J.P., 2009. Methane and carbon dioxide sorption and transport rates in coal at In-situ conditions. Energy Procedia, *In Press.*
4. Pone, J.D.N., Halleck, P.M., Mathews, J.P., 2009. Characterization of coal matrix deformation for sequestration and enhanced coalbed methane recovery at in-situ stress conditions. International Journal of Coal Geology, submitted.
5. Pone, J.D.N., Halleck, P.M., Mathews, J.P., 2009. Kinetic modeling of the sorption of carbon dioxide on powder and non-powder bituminous coal for sequestration and enhanced coalbed methane recovery. SPE Annual Technical Conference and Exhibition (ATCE) 2009, 4–7 October, in New Orleans, Louisiana.

In all cases, first-authorship establishes my principal role in developing and executing the analysis.

References

Anderson, R.B., Hall, W.K., Lecky, J.A. and Stein, K.C., 1956. Sorption studies on American coals. Journal of Physical Chemistry, 60(11): 1548-1558.

Brenner, D., 1983. The macromolecular states of solvent-swollen and dry coal. Nature, 306(22/29): 772-773.

Brenner, D., 1985. The macromolecular nature of bituminous coal. Fuel, 64(2): 167-173.

Brown, T.D., Harrison, D.K., Jones, J.R. and LaSota, K.A., 2007. Recovering coal bed methane from deep unmineable coal seams and carbon sequestration. International Journal of Environment and Pollution, 29(4): 474-483.

Busch, A., Gensterblum, Y., Krooss, B.M. and Littke, R., 2004. Methane and carbon dioxide adsorption-diffusion experiments on coal: upscaling and modeling. International Journal of Coal Geology, 60(2-4): 151-168.

Harpalani, S. and Chen, G., 1997. Influence of gas production induced volumetric strain on permeability of coal. Geotechnical and Geological Engineering, 15(4): 303-325.

Holloway, S., 2005. Underground sequestration of carbon dioxide--a viable greenhouse gas mitigation option. Energy, 30(11-12): 2318-2333.

IPCC, 2005. Carbon Dioxide Capture and Storage: Special Report of the Intergovernmental Panel on Climate Change. Cambridge University Press.

Karacan, C.O., 2003. Heterogeneous sorption and swelling in a confined and stressed coal during CO_2 injection. Energy & Fuels, 17(6): 1595-1608.

Kini, K.A., Nandi, S.P., Sharma, J.N., Iyengar, M.S. and Lahiri, A., 1956. Surface area of coal. Fuel, 35(1): 71-76.

Levine, D.G., Schosberg, R.H., Silbernagel, B.G, 1982. Understanding the chemistry and physics of coal structure (A Review). Proceedings of the National Academy of Sciences of the United States of America, 79(10): 3365-3370.

Mazumder, S., Karnik, A. and Wolf, K.H., 2006. Swelling of coal in response to CO_2 sequestration for ECBM and its effect on fracture permeability. SPE Journal, 97754: 390-398.

Nandi, S.P., Kini, K.A. and Lahiri, A., 1956. Adsorption of polar gases by anthracite. Fuel, 35(1): 133-134.

Shi, J.Q. and Durucan, S., 2005. CO_2 storage in deep unminable coal seams. Oil & Gas Science and Technology - Rev. IFP, 60(3): 547-558.

Stopes, M.C., 1919. On the four visible ingredients in banded bituminous coal studies in the composition of coal, no 1. Proceedings of the Royal Society of London Series B-Containing Papers of a Biological Character, 90(632): 470-487.

Tideswell, F.V. and Wheeler, R.V., 1919. A chemical investigation of banded bituminous coal - Studies in the composition of coal. Journal of the Chemical Society, 115: 619-636.

Walker, P.L., Verma, S.K., Rivera-Utrilla, J. and Khan, M.R., 1988. A direct measurement of expansion in coal and macerals induced by carbon dioxide and methanol, Fuel, 1988, 67, 719. Fuel, 67: 719-728.

White, C.M. et al., 2005. Sequestration of carbon dioxide in coal with enhanced coalbed methane recovery - A review. Energy and Fuels, 19(3): 659-724.

Chapter 2

Detailed 3D Characterization of Coal Strains Induced by Compression, Carbon Dioxide Sorption, and Desorption at Simulated in-situ Conditions

Abstract

Sequestration of carbon dioxide in unmineable coal seams is an option to combat climate change and an opportunity to enhance coalbed methane production. Prediction of sequestration potential requires characterization of porosity, permeability, sorption capacity and the magnitude of swelling due to carbon dioxide uptake or shrinkage due to methane and water loss. Available reservoirs simulators of the sorption and transport of gases in coal require such data. Unfortunately, the majority of data characterizing coal-gas systems have been obtained from powdered, unconfined coal samples. Little is known about confined coal behavior during carbon dioxide uptake and methane desorption. The present work focuses on the characterization of coal regional compression, and strain behavior during CO_2 uptake at simulated in-situ conditions. It includes the evaluation of three-dimensional strain induced by the confining stress and the sorption and desorption of carbon dioxide. X-ray computer tomography allowed three-dimensional characterization of the bituminous coal deformation samples under stress. The application of 6.9MPa of confining stress contributes an average of -0.34% volumetric strain. Normal strains due to confining stress were -0.08%, -0.15% and -0.11% along the x,y and z axes respectively. Confined coal exposed to CO_2 for 26 days displays an average volumetric expansion of 0.4%. Normal strains due to CO_2 sorption

were 0.11%, 0.22% and 0.11% along x,y and z axes. Drainage of the CO_2 induced an average of -0.33% volumetric shrinkage. Normal strains due to CO_2 desorption were -0.23%, -0.08% and -0.02% along x, $y$and z axes. Three-dimensional region specific strain distribution along with magnitude of deformation induced by carbon dioxide is presented and discussed.

Introduction

For a successful sequestration of carbon dioxide in coal seams and subsequent enhanced coalbed methane recovery (ECBM), knowledge of coal structural properties and their variation under replicated in-situ stress conditions is required (Holloway, 1997; Wang et al., 2007; White et al., 2005). Reliable data characterizing dynamic coal behavior is desirable for the development and management of coal seam CO_2 sequestration projects. Prediction of the influence of coal heterogeneities and resultant strain distributions is challenging due to the chemical and physical processes occurring during CO_2 sequestration. Simplistic modeling approaches of coal shrinkage and swelling based on conventional volumetric methods do not adequately represent coal behavior (Wang et al., 2007). Thus, there is a gap between data required for constitutive models and the current ability of experimental mechanics to provide this information. Analytical methods should account for anisotropy, heterogeneity, non-linearity in the structure behavior that may include: compression, compaction, softening, collapse, and rebound phenomena. Coal seams are being investigated for sequestration applications because they exhibit desirable material properties, such as high sorption capacity, high porosity or

high specific surface areas (Walker, 1981; Walker et al., 1988a; Walker and Mahajan, 1993). However, these same characteristics also make the prediction of the material response difficult especially when dealing with plasticity and structure changes (rearrangement). To achieve the full potential of coal seams to sequester CO_2, they must be well characterized with predictive models. Therefore, it is desirable to provide detailed information about the coal deformation characteristics.

The analysis of rock behavior in 3D has advanced with X-ray Computed Tomography (CT) 3D data sets at micrometer scale (de Oliveira et al., 2003; Denison and Carlson, 1997; Denison et al., 1997). High-resolution computed tomography has been used to study the architectural details of materials (Maire et al., 2007). There have also been applications in more traditional engineering and physicals science settings (Duliu et al., 2003; Gualda and Rivers, 2006; Kohjiya et al., 2005). It has been used as a nondestructive inspection tool for the visualization of internal flaws and damage and for the identification of internal material heterogeneities (Krimmel et al., 2005; Ren and Ge, 2004). Evaluations have included the measurement of permeability, gas sorption capacity within geological samples, and the visualization of internal cracks within samples under stress (Kantzas, 1990; Karacan, 2003; Nakashima and Kamiya, 2007; Raynaud et al., 1989; Van Geet and Swennen, 2001; Van Geet et al., 2000).

In contrast to conventional radiography projection, in which a two-dimensional projection of a three-dimensional object is made, computed tomography reconstructs a volume rendering from which volumetric reconstruction can be generated and cross-sectional views of selected transverse planes obtained. The CT imaging allows a quantitative map of the X-ray attenuation throughout the sample. The distribution of the

X-ray attenuation coefficients allows the localization of specific features in the material. Following the displacement of these features throughout the volume permits strain evaluations. This technique quantifies the microstructure deformation and any heterogeneous behavior.

In-situ strain calculation was initially based upon reconstructions of two-dimensional photo-elasticity images (Barbone and Bamber, 2002; Vacher et al., 1999) or upon numerical modeling (Glover et al., 1996; Li, 1995; Liu, 1982; Vukadin, 2007) which has been extended to 3D CT images to improve structure behavior predictions in geomaterials (Alshibli and Al-Hamdan, 2001; Alshibli and Hasan, 2008; Alshibli et al., 2000; Mazumder et al., 2006b; Raynaud et al., 1989; Van Geet and Swennen, 2001). Furthermore, by enabling a direct visualization of the dynamic behavior of rock microstructures, CT studies contribute to improved description of swelling/compaction mechanisms or flow properties during fluid uptake. Previous workers have contributed to improved strain distribution and fluid transport evaluation based on CT data (Kantzas, 1990). Several approaches exist to quantify structure deformation from CT data. They can be roughly classified in two categories: digital volume correlation of images collected at different strain state conditions (Bay et al., 1999; Bruck, 1989; Kang et al., 2007; Louis et al., 2006; Smith and Bay, 2001; Smith et al., 2002; Verhulp et al., 2004) and features tracking (Kobayashi et al., 2007; Ohgaki et al., 2006; Toda et al., 2007). Features tracking method is appropriate for coal specimens because of the low CT image contrast and the presence of high density material (mineral grains) which can be tracked. The estimation of 3D strain distribution in coal using an accurate tracking method based on finite element approach was developed and applied to characterize the behavior of

bituminous coal in 3D. An assessment of the three-dimensional local strain distribution induced in coal structure due to stress application, CO_2 uptake and desorption based on the analysis of high-resolution industrial X-ray computed tomography images is presented.

Material and Method

This paper applies a three-dimensional full-field measurement technique, based on high-resolution X-ray computed tomography, to quantify strains and visualize deformation in a bituminous coal core. The basic sequence for application of tracking method to strain field measurements involves three mains steps: (1) generation of volume images of sample in original and altered states; (2) measurement of a discrete displacement vector field throughout the sample by features tracking procedure; and finally (3) calculation of the strain tensor field from the measured displacement vector field.

Sample Preparation

A coal core was prepared from a coal block collected from the Hazard No. 9 coal seam, Perry County, Western Kentucky. The highwall overburden, mostly sandstone was estimated to be 160 feet thick and the seam to be 4 feet thick. The block was removed and coated with water-based Polycrylic protective finish to prevent any further oxidation or drying of the sample and it was also cast in plaster to aid the coring process. A 1 inch

diameter and 2.5 inches length core was obtained parallel to the bedding plane. The core was preserved in sealed container under nitrogen until use. The end surfaces were polished to produce a flat and parallel surface for stress application and gas flow distribution. Once mounted in the core holder, the sample was evacuated by applying a vacuum of < 100 μm of Hg for 48 hours. Experiments were conducted under controlled temperature of 20ºC ± 0.5. A reference scan was obtained before the stress application. To simulate a potential 1000 feet deep sequestration site, an arbitrary confining stress of 6.8 MPa (1000 psi) confining stress was applied to the sample. A period of 48 hours was allows for stress equilibrium. After 26 days of multi-dosing injection of CO_2 the sample was again scanned to evaluate the impact of the sorption on the structure. The sample was also scanned after 15 days of multi-steps desorption to assess shrinkage.

CT Images Acquisition

The unconfined and confined core was analyzed using X-ray CT technology. Four sets of scans of the sample were taken: (1) evacuated sample at unconfined state, (2) subjected to confining pressure for 48 hours before exposed to CO_2 , (3) subjected to confining pressure and after 26 days of exposure to CO_2, and (4) subjected to confining pressure after 15 days of CO_2 desorption. Scans were analyzed at voxel resolutions of 0.026 x 0.026 x 0.032 mm for x, y, and z dimensions. Figure 2-1a shows a volume rendering of the core. The image is shown on a gray scale. Light shades represent material of high X-ray attenuation (relative high density) and dark shades represent material of low X-ray attenuation (relative low density). The white layers represent

mineral bands which have a relative high X-ray attenuation. A more descriptive discussion of similar volumetric renderings could be found elsewhere (Hile, 2006; Karacan and Mitchell, 2003).

Quantitative Analysis of CT Images

The CT scans were viewed and analyzed using commercial software. After volume rendering, multiple mineral grains (fuducials) were located to generate regional tetrahedron element in each volume. Some 43 tetrahedrons were constructed. The strain obtained from the deformation of the tetrahedron was represented at its centroid. The coordinates of these fuducials in successive scans were located (Figure 2-1b). The same fuducials were identified in both volume sets. The coordinates of the centroid of the fuducials were calculated for the two successive scans. The translation in any direction can be calculated as the difference between the location of the fuducial initially and its location after the stress condition [Eqs. (1)- (3)], and the distance traveled by the fuducial can be evaluated using Eq. (4). The regional strain is then calculated from the deformation of each tetrahedron.

$$\Delta x = x_{(scan2)} - x_{(scan1)} \quad (1)$$

$$\Delta y = y_{(scan2)} - y_{(scan1)} \quad (2)$$

$$\Delta z = z_{(scan2)} - z_{(scan1)} \quad (3)$$

$$D = \sqrt{\Delta x^2 + \Delta y^2 + \Delta z^2} \quad (4)$$

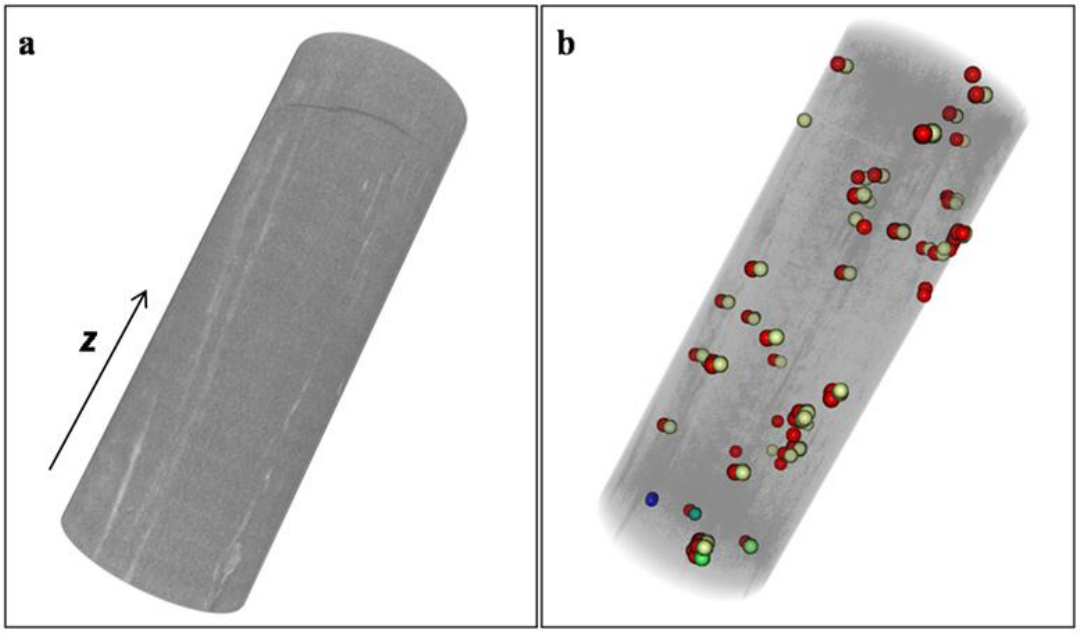

Figure 2-1: a) Volume rendering of coal core; b) Fuducials positions at two different stress states on the coal core; red indicating the position before and green after stress application.

Fuducials Tracking Method and Strain Calculation

The state of the displacement of a point is defined by three directional displacement components u, v, and w, in directions x, y, and z. Fiducials's coordinates from the first CT scan were group in four immediate neighbors representing a strain element (Figure 2-1). Figure 2-2 illustrates a tetrahedral element i, j, m, p in space defined by the three coordinates x, y and z where i, j, m, p are the indices of the four fuducials. Several sets of four fuducials were used to evaluate the resulting strain at the centroid of the tetrahedral due to the application of the confining stress, due to CO_2 uptake and finally due to CO_2 desorption.

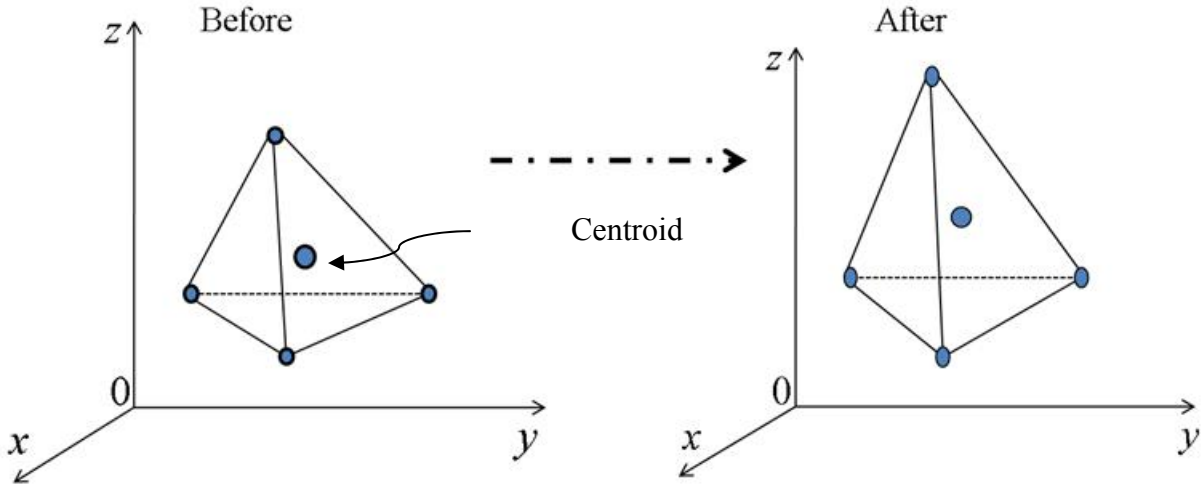

Figure 2-2: A tetrahedral of fuducials, used as a strain element, and the volumetric centroid point of the representation of the resulting strain. "Before" shows the configuration of fuducials before the application of stress.

The displacement of a node has three components

$$a_i = \begin{pmatrix} u_i \\ v_i \\ w_i \end{pmatrix} \tag{5}$$

The displacements within an element have to be uniquely defined by the three linear polynomials as described by Zienkiewicz and Taylor (1989):

$$u = \alpha_1 + \alpha_2 x + \alpha_3 y + \alpha_4 z \tag{6}$$

$$v = \alpha_5 + \alpha_6 x + \alpha_7 y + \alpha_8 z \tag{7}$$

$$w = \alpha_9 + \alpha_{10} x + \alpha_{11} y + \alpha_{12} z \tag{8}$$

The twelve constants α can be determined by solving the three sets of four simultaneous equations which arise when the nodal coordinates are inserted and the displacements equated to the appropriate nodal displacements. Having the coordinates and displacements of four fuducials, the system of equations can be written as:

$$u_i = \alpha_1 + \alpha_2 x_i + \alpha_3 y_i + \alpha_4 z_i \tag{9}$$

$$u_j = \alpha_1 + \alpha_2 x_j + \alpha_3 y_j + \alpha_4 z_j \tag{10}$$

$$u_m = \alpha_1 + \alpha_2 x_m + \alpha_3 y_m + \alpha_4 z_m \tag{11}$$

$$u_p = \alpha_1 + \alpha_2 x_p + \alpha_3 y_p + \alpha_4 z_p \tag{12}$$

From which α_1 to α_4 can be evaluated. The solution of this system of equations can be rewritten in more general form using determinant form as follows (Zienkiewicz and Taylor, 1989):

$$u = \frac{1}{6V}\left[(a_i + b_i x + c_i y + d_i z)u_i + \left(a_j + b_j x + c_j y + d_j z\right)u_j + (a_m + b_m x + c_m y + d_m z)u_m + \left(a_p + b_p x + c_p y + d_p z\right)u_p\right] \tag{13}$$

$$v = \frac{1}{6V}\left[(a_i + b_i x + c_i y + d_i z)v_i + \left(a_j + b_j x + c_j y + d_j z\right)v_j + (a_m + b_m x + c_m y + d_m z)v_m + \left(a_p + b_p x + c_p y + d_p z\right)v_p\right] \tag{14}$$

$$w = \frac{1}{6V}\left[(a_i + b_i x + c_i y + d_i z)w_i + \left(a_j + b_j x + c_j y + d_j z\right)w_j + (a_m + b_m x + c_m y + d_m z)w_m + \left(a_p + b_p x + c_p y + d_p z\right)w_p\right] \tag{15}$$

$$\text{With } V = \frac{1}{6}\det\begin{vmatrix} 1 & x_i & y_i & z_i \\ 1 & x_j & y_j & z_j \\ 1 & x_m & y_m & z_m \\ 1 & x_p & y_p & z_p \end{vmatrix} \tag{15a}$$

The value of V represents the volume of the tetrahedron. By expanding the other relevant determinants into their co-factors we have:

$$a_i = \det\begin{vmatrix} x_i & y_i & z_i \\ x_m & y_m & z_m \\ x_p & y_p & z_p \end{vmatrix}; \qquad b_i = -\det\begin{vmatrix} 1 & y_j & z_j \\ 1 & y_m & z_m \\ 1 & y_p & z_p \end{vmatrix} \tag{15b}$$

$$c_i = -\det\begin{vmatrix} x_j & 1 & z_j \\ x_m & 1 & z_m \\ x_p & 1 & z_p \end{vmatrix}; \qquad d_i = -\det\begin{vmatrix} x_j & y_j & 1 \\ x_m & y_m & 1 \\ x_p & y_p & 1 \end{vmatrix}$$

With the other constant defined by cyclic interchange of the subscripts in the order $p, i, j \; and \; m$.

Strains were calculated using Lagrangian description defined by Eq. (16) - Eq. (18). They were calculated with reference to the initial state for that set.

$$\varepsilon_x = \frac{\partial u}{\partial x} \tag{16}$$

$$\varepsilon_y = \frac{\partial v}{\partial y} \tag{17}$$

$$\varepsilon_z = \frac{\partial w}{\partial z} \tag{18}$$

The volumetric strain was defined as:

$$\varepsilon_v = \varepsilon_x + \varepsilon_y + \varepsilon_z \quad (19)$$

The procedure was repeated for the entire strain elements (tetrahedrons) in the volume, yielding local strain values that allows the characterization of coal core in three dimensions. Tetrahedrons boundaries were shared as recommended by Alshibli (2006) to ensure continuity of strain calculations.

Result and Discussion

Swelling induced by CO_2 sorption impacts strain distribution on the coal core. Measurements of three-dimensional local strain distribution showed that the introduction of CO_2 in confined coal contributes to both local compression and dilation in the x, y and z directions. Results are summarized in Table 2-1 and Figures 2-3 to 2-8. The negative values indicate compression while the positive values indicate the dilation.

TABLE 2.1: Normal and volumetric strains induced in bituminous coal core by the confining stress, the sorption of CO_2 and the desorption of CO_2 respectively

	ε_x (%)	(%)	ε_z (%)		ε_v (%)	
Average	-0.08	0.15	-0.11		-0.34	Compression induced by 1000 psi confining stress
MIN	-3.37	3.09	-2.20		-7.29	
MAX	0.86	.80	0.41		0.61	
Average	0.11	.22	0.11		0.44	Swelling induced by the sorption of CO_2 under 1000 psi confining stress
MIN	-1.24	0.89	-0.88		-1.76	
MAX	2.63	.40	2.05		2.52	

Average	-0.23	0.08	-0.02		-0.33	Shrinkage induced by the desorption of CO_2 under confining stress
MIN	-2.21	1.13	-0.82		-2.35	
MAX	0.44	.55	0.60		0.60	

Table 2.1 shows an average volumetric compression of -0.34% due to 6.9MPa confining stress. The introduction of CO_2 leads to an average volumetric swelling of 0.44%. Desorption of CO_2 contributes to an average volumetric compression of -0.33. The swelling of the matrix during sorption is not balance by the shrinkage after desorption. This result confirms that the deformation of coal structure due to CO_2 sorption is irreversible as noted by Briggs and Sinha (1932). Also that coal swells even under confining stress (Karacan, 2007; Karacan, 2003; Mathews et al., 2001)

Figure 2-3 shows the variation of normal strain along the sample longitudinal profile (z axis) due to confining stress. Compression and expansion occurs throughout the sample. From Figures 2-3, ε_x varies from -3.4% compression to 0.9% swelling; the values of ε_y range from -3.0% to 0.8%; and ε_z values range from -2.2% to 0.4%. The maximum compression occurs in the plane containing x and y. Maximum deformation should be expected on the plane perpendicular to the bedding plane as suggested by previous workers (Gorbaty et al., 1986; Larsen, 1988). Figure 2-4 shows the variation of the volumetric strain along the sample longitudinal profile due to the confining stress.

Figure 2-4 shows that 6.8 MPa confining stress contributes to an average volumetric strain of -0.3%, indicating a net compression as expected.

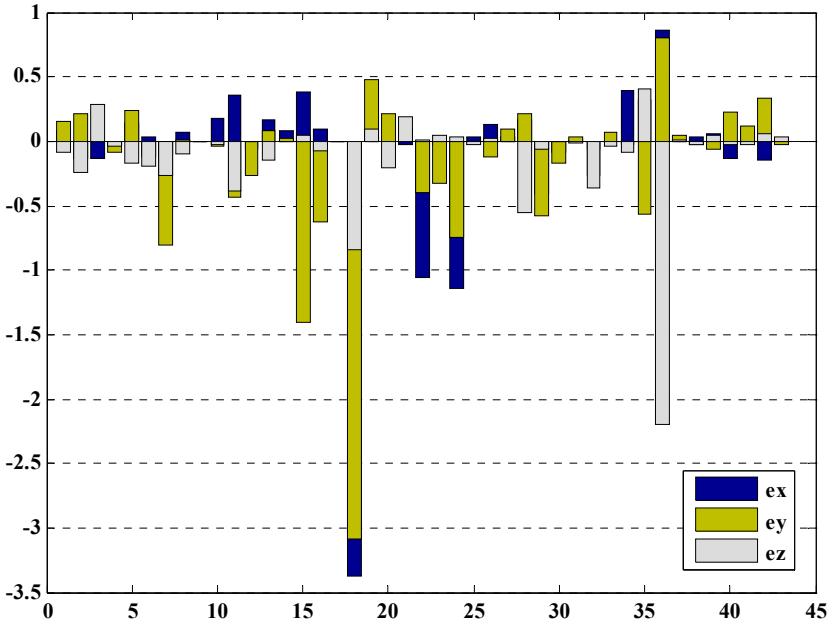

Figure 2-3: Normal strains induced in a bituminous coal core by 1000 psi confining stress before CO_2 exposure

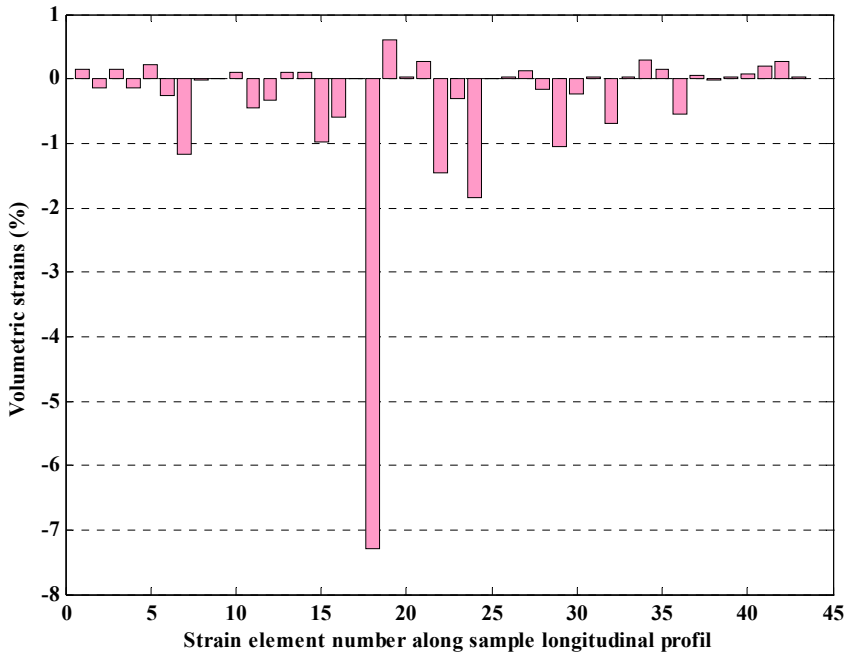

Figure 2-4: Volumetric strain induced in a bituminous coal core by 1000 psi confining stress before CO_2 exposure

Figures 2-5 and 2-6 shows the normal and volumetric swelling of coal due to CO_2 uptake. Strain in the x direction, ε_x , varies from -1.2% compression to 2.6% swelling; the values of ε_y range from -0.9 % to 2.4%; and ε_z values range from -0.9% to 2.0%. The maximum swelling occurs as during the compression on the x and y axis. The average volumetric strain for the whole sample is 0.4 % which indicates a net expansion of the coal structure due to CO_2 exposure. Normal and volumetric strain values obtained are comparable with other work (See Table 2-2) (Chikatamarla et al., 2004; Gray, 1987; Levine, 1996; Mazumder et al., 2006a; Moffat and Weale, 1955; Reucroft, 1987; Reucroft and Patel, 1986; Robertson and Christiansen, 2005; Seidle and Huitt, 1995;

Walker et al., 1988b; Zutshi and Harpalani, 2004) although higher values have been obtained also for unconfined coals.

Table 2-2: Coal strains induced by CO_2 sorption as reported by various workers

Strain		Source
Type	**Value (%)**	
Longitudinal	0.57	Briggs and Sinha, 1932
Longitudinal	0.5	Mofat and Weale 1955
Longitudinal	1.0	Gray, 1987
Longitudinal	0.8	Seidle and Huitt, 1995
Longitudinal	0.5	Levine, 1996
Volumetric	1.1	Zutshi and Harpalani, 2004
Volumetric	2.41	Chikatamarla et al., 2004
Longitudinal	0.5 - 1.3	Robertson and Christiansen, 2005
Volumetric	1.48	Mazumder et al., 2006

Table 2.2 summarizes coal strain data collected using dilatometer or resistance-type strain. Strain values reported are not directly comparable because of different experimental conditions coals. However, these data do show that average CO_2 sorption-induced strain presented in this paper is relatively low compare to reported values in the literature. This is likely due to the confining stress.

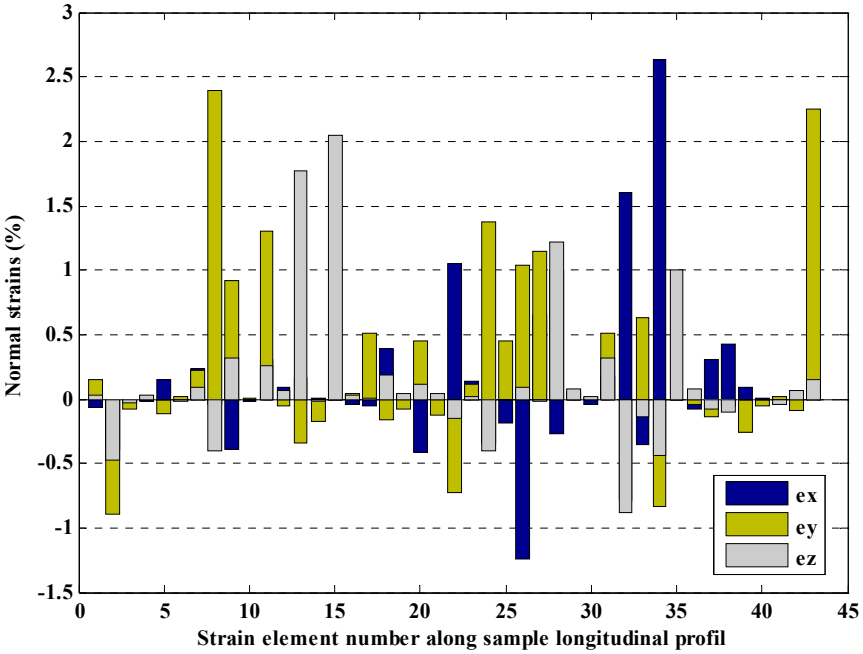

Figure 2-5: Normal strains induced in a bituminous coal core by the sorption of CO_2 at 1000 psi confining stress.

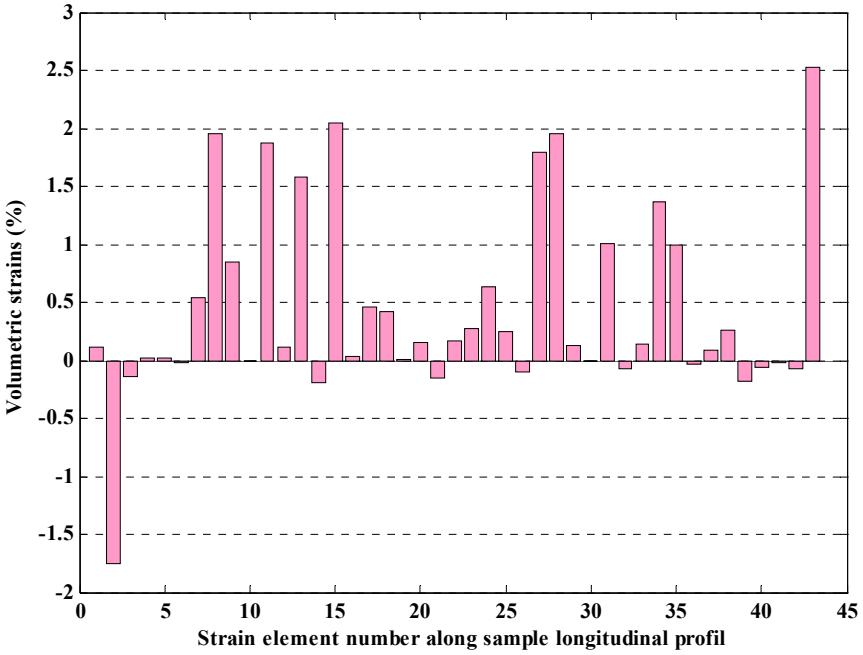

Figure 2-6: Volumetric strain induced on bituminous coal core by the sorption of CO_2 at 1000 psi confining stress.

Figure 2-7 and 2-8 shows the normal and volumetric strains of coal due to CO_2 desorption. ε_x varies from -2.2% compression to 0.4% swelling; the values of ε_y range from -1.1 % to 0.5%; finally ε_z values range from -0.8% to 0.6%. The volumetric strain varies from -2.3% to 0.6% with an average of -0.3%. A net contraction/compression with the CO_2 release as expected.

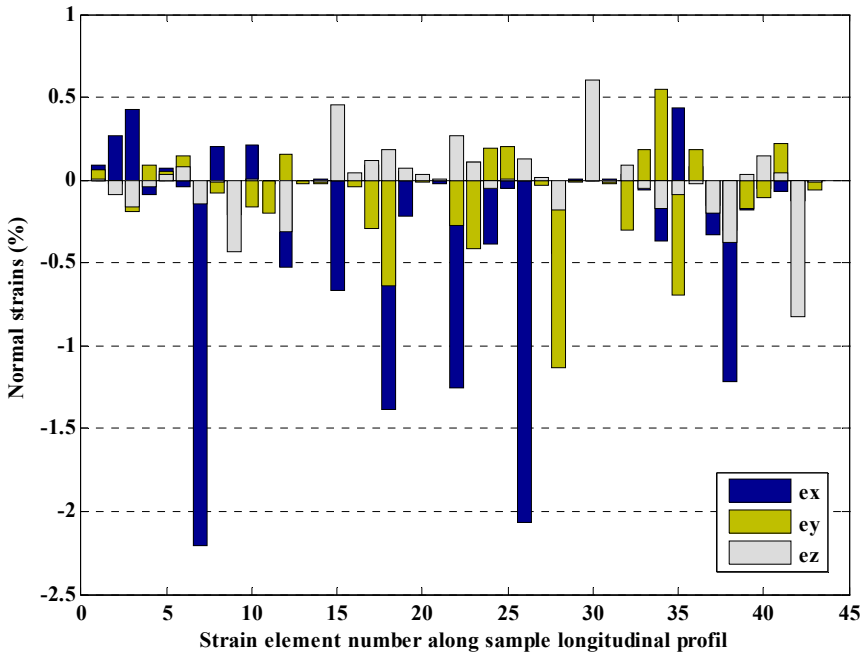

Figure 2-7: Normal strains induced in a bituminous coal core at 1000 psi confining stress by the desorption of CO_2 to atmospheric pressure.

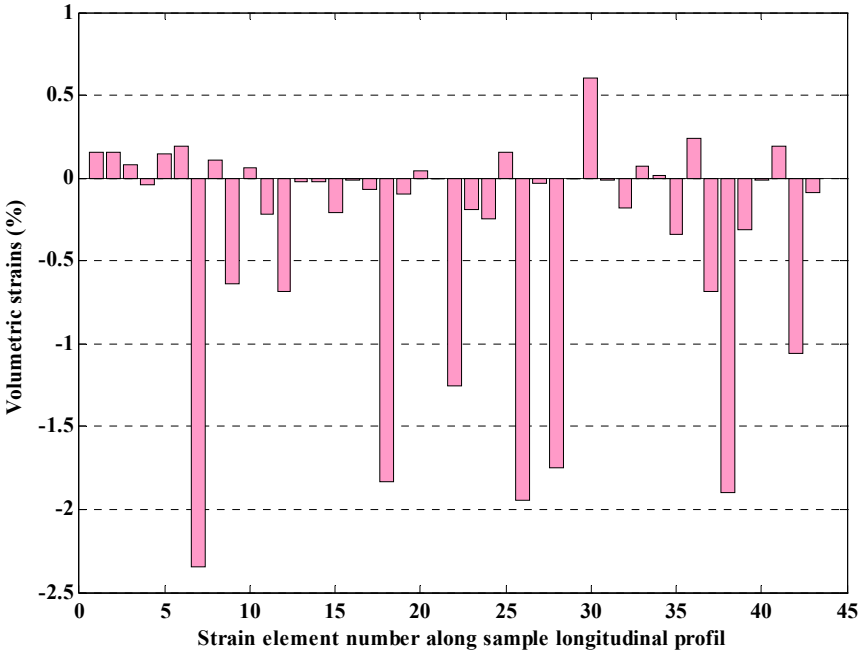

Figure 2-8: Volumetric strain induced in a bituminous coal at 1000 psi confining stress by the desorption of CO_2 to atmospheric pressure.

Lithotypes constituting the coal structure display different chemical and physical characteristics (Fitzgerald and Vankrevelen, 1959; Scott, 2002). This contributes to the non-uniform sorption kinetic and capacity (Gorbaty et al., 1986; Karacan, 2003). Therefore, it is likely that some of the lithotypes band in coal are compressed or compacted to accommodate the swelling of an adjacent lithotype.

The results from the uniaxial testing undertaken by Viete and Ranjith (2006) suggest that CO_2 adsorption has a softening effect on coal. A similar result was reported by Mehic et al. (2006). Any weakening of the coal under confining stress will contribute compression. Alternating positive and negative values of the strain could be explained by the heterogeneity of coal. It would have not been expected for powdered or unconfined coal. Non-uniform deformation can result from kinetic effects or from differences in the

extent of swelling of the various microscopic subcomponents of coal (Gorbaty et al., 1986). Bituminous coal often has a layered structure of different lithotypes which have different chemical composition. Kinetic effects occur because macerals constituting those lithotypes are penetrated by carbon dioxide at different rates or because they swell at different rates. The expansion of the more accessible regions (fractures and cleats) of coal due to high pore pressure will produce large stresses when constrained by confining stress, potentially compressing adjacent regions. Coal macerals and mineral matter have different swelling extents, hardnesses, and morphology, all of which contribute to localized stresses and deformations as swelling proceeds. Coal is not isotropic and models developed on this basis can be improved. In spite of an extensive recent literature in characterizing coal for CO_2 sequestration, significant gaps in knowledge still exist.

Conclusion

The feature tracking method for three dimensional strain calculations has been successfully used to quantify the deformation of coal during confining stress application, CO_2 sorption and desorption. The combination of the high resolution CT data and the fuducials tracking provides the three-dimensional information of local strain distribution and allows investigating relationship between microstructure and local deformation. The application of 6.9MPa of confining stress contributes an average -0.34% volumetric strain. Normal strains due to confining stress observed were -0.08%, -0.15% and -0.11% along x, y and z axes. Confined coal and exposed to CO_2 for almost a month displays an average volumetric expansion of 0.4% although, locally regions compressed or swelled.

Normal strains due to CO_2 sorption were 0.11%, 0.22% and 0.11% along x, y and z axes. Desorption of the CO_2 to atmospheric pressure induced an average -0.33% volumetric shrinkage. Normal strains due to CO_2 desorption were -0.23%, -0.08% and -0.02% along x, y and z axes. Swelling of coal during sorption was not balance by the shrinkage after CO_2 release. Coal swelled even under these confining stresses. Alternating positive and negative strain values observed during compression, sorption and desorption respectively emphasized that compression/compaction and expansion of coal will occur during CO_2 sequestration. Improved representation of the physical state of coal is needed to better characterize and utilize unmineable coal seams as sequestration sites.

Acknowledgements

Glenn Stracher and James Hower for their help in sample collection.

Reference

Alshibli, K.A. and Al-Hamdan, M.Z., 2001. Estimating volume change of triaxial soil specimens from planar images. Computer-Aided Civil and Infrastructure Engineering, 16(6): 415-421.

Alshibli, K.A., Alramahi, B.A., 2006. Microscopic evaluation of strain distribution in granular materials during shear. Journal of Geotechnical and Geoenvironmental Engineering, 132(1): 80-91.

Alshibli, K.A. and Hasan, A., 2008. Spatial variation of void ratio and shear band thickness in sand using X-ray computed tomography. Geotechnique, 58(4): 249-257.

Alshibli, K.A. et al., 2000. Assessment of localized deformations in sand using X-ray computed tomography. Geotechnical Testing Journal, 23(3): 274-299.

Barbone, P.E. and Bamber, J.C., 2002. Quantitative elasticity imaging: what can and cannot be inferred from strain images. Physics in Medicine and Biology, 47(12): 2147-2164.

Bay, B.K., Smith, T.S., Fyhrie, D.P. and Saad, M., 1999. Digital volume correlation: Three-dimensional strain mapping using X-ray tomography. Experimental Mechanics, 39(3): 217-226.

Briggs, H. and Sinha, R.P., 1932. Expansion and contraction of coal caused respectively by sorption and discharge of gas. Proceedings of the Royal Society of Edinburgh, 53(1): 48-53.

Bruck, H.A., McNeill, S.R., Sutton, M.A., Peters III, W.H., 1989. Digital image correlation using New-Raphson method of partiel differential correction. Experimental Mechanics, 29(3): 261-267.

Chikatamarla, L., Cui, X. and Bustin, R.M., 2004. Implications of volumetric swelling/shrinkage of coal in sequestration of acid gases, International Coalbed Methane Conference, Tuscaloosa, AL, pp. 0435.

de Oliveira, L.F., Lopes, R.T., de Jesus, E.F.O. and Braz, D., 2003. 3D X-ray tomography to evaluate volumetric objects. Nuclear Instruments & Methods in Physics

Research Section a-Accelerators Spectrometers Detectors and Associated Equipment, 505(1-2): 573-576.

Denison, C. and Carlson, W.D., 1997. Three-dimensional quantitative textural analysis of metamorphic rocks using high-resolution computed X-ray tomography 2. Application to natural samples. Journal of Metamorphic Geology, 15(1): 45-57.

Denison, C., Carlson, W.D. and Ketcham, R.A., 1997. Three-dimensional quantitative textural analysis of metamorphic rocks using high-resolution computed X-ray tomography 1. Methods and techniques. Journal of Metamorphic Geology, 15(1): 29-44.

Duliu, O.G., Rizescu, C.T. and Ricman, C., 2003. Dual energy gamma-ray axial computer tomography investigation of some metamorphic and sedimentary rocks. Neues Jahrbuch Fur Geologie Und Palaontologie-Abhandlungen, 228(3): 343-362.

Fitzgerald, D. and Vankrevelen, D.W., 1959. Chemical structure and properties of coal . The kinetics of coal carbonization. Fuel, 38(1): 17-37.

Glover, P.W.J. et al., 1996. Modelling the stress-strain behaviour of saturated rocks undergoing triaxial deformation using complex electrical conductivity measurements. Surveys in Geophysics, 17(3): 307-330.

Gorbaty, M.L., Mraw, S.C., Gethner, J.S. and Brenner, D., 1986. Coal physical structure: porous rock and macromolecular network. Fuel Processing Technology, 12: 31-49.

Gray, I., 1987. Reservoir engineering in coal seams: Part 1 - The physical process of gas storage and movement in coal seams. SPE, 12514.

Gualda, G.A.R. and Rivers, M., 2006. Quantitative 3D petrography using X-ray tomography: Application to Bishop Tuff pumice clasts. Journal of Volcanology and Geothermal Research, 154(1-2): 48-62.

Hile, L.M., 2006. CO_2 sorption by Pittsburgh-seam coal subjected to confining pressure. Master Thesis, The Pennsylvania State University, University Park.

Holloway, S., 1997. An overview of the underground disposal of carbon dioxide. Energy Conversion and Management, 38(Supplement 1): S193-S198.

Kang, J., Ososkov, Y., Embury, J.D. and Wilkinson, D.S., 2007. Digital image correlation studies for microscopic strain distribution and damage in dual phase steels. Scripta Materialia, 56(11): 999-1002.

Kantzas, A., 1990. Investigation of physical-properties of porous rocks and fluid-flow phenomena in porous-media using computer-assisted tomography. In Situ, 14(1): 77-132.

Karacan, C.O., 2007. Swelling-induced volumetric strains internal to a stressed coal associated with CO_2 sorption. International Journal of Coal Geology, 72(3-4): 209-220.

Karacan, C.O. and Mitchell, G.D., 2003. Behavior and effect of different coal microlithotypes during gas transport for carbon dioxide sequestration into coal seams. International Journal of Coal Geology, 53(4): 201-217.

Karacan, O.C., 2003. An effective method for resolving spatial distribution of adsorption kinetics in heterogeneous porous media: Application for carbon dioxide sequestration in coal. Chemical Engineering Science, 58(20): 4681-4693.

Kobayashi, M. et al., 2007. Three-dimensional measurement of local strain distribution by tracking microstructural features in high-resolution SR-CT image. Key Engineering Materials, 345-346: 1153-1156.

Kohjiya, S., Katoh, A., Shimanuki, J., Hasegawa, T. and Ikeda, Y., 2005. Three-dimensional nano-structure of in situ silica in natural rubber as revealed by 3D-TEM/electron tomography. Polymer, 46(12): 4440-4446.

Krimmel, S., Stephan, J. and Baumann, J., 2005. 3D computed tomography using a microfocus X-ray source: Analysis of artifact formation in the reconstructed images using simulated as well as experimental projection data. Nuclear Instruments & Methods in Physics Research Section a-Accelerators Spectrometers Detectors and Associated Equipment, 542(1-3): 399-407.

Larsen, J.W., 1988. Macromolecular structure and coal pyrolysis. Fuel Processing Technology, 20: 13-22.

Levine, J.R., 1996. Model study of the influence of matrix shrinkage on absolute permeability of coal bed reservoirs In: R. Gayer and I. Harris (Editors), Coalbed Methane and Coal Geology. Geological Society Special Publication, pp. 197-212.

Li, C.L., 1995. Micromechanics modeling for stress-strain behavior of brittle rocks. International Journal for Numerical and Analytical Methods in Geomechanics, 19(5): 331-344.

Liu, J., 1982. The numerical-method for analyzing the deformation and failure of rocks based on the stress-strain curve group. Scientia Geologica Sinica(1): 103-110.

Louis, L., Wong, T.-f., Baud, P. and Tembe, S., 2006. Imaging strain localization by X-ray computed tomography: discrete compaction bands in Diemelstadt sandstone. Journal of Structural Geology, 28(5): 762-775.

Maire, E., Colombo, P., Adrien, J., Babout, L. and Biasetto, L., 2007. Characterization of the morphology of cellular ceramics by 3D image processing of X-ray tomography. Journal of the European Ceramic Society, 27(4): 1973-1981.

Mathews, J.P., Karacan, O., Halleck, P., Mitchell, G.D. and Grader, A., 2001. Storage of pressurized carbon dioxide in coal observed using X-Ray tomography. First National Conference on Carbon Sequestration, 2001, Washington, DC, Online at: http://www.netl.doe.gov/publications/proceedings/01/carbon_seq/7a4.pdf.

Mazumder, S., Karnik, A. and Wolf, K.H., 2006a. Swelling of coal in response to CO_2 sequestration for ECBM and its effect on fracture permeability. SPE Journal, 97754: 390-398.

Mazumder, S., Wolf, K.H.A.A., Elewaut, K. and Ephraim, R., 2006b. Application of X-ray computed tomography for analyzing cleat spacing and cleat aperture in coal samples. International Journal of Coal Geology, 68(3-4): 205-222.

Mehic, M., Ranjith, P.G., Choi, S.K. and Haque, A., 2006. The geomechanical behavior of Australian black coal under the effects of CO_2 injection: Uniaxial testing. Geotechnical Special Publication. American Society of Civil Engineers, Reston, VA 20191-4400, United States, Shanghai, China, pp. 290-297.

Moffat, D.H. and Weale, K.E., 1955. Sorption by coal of methane at high pressures. Fuel, 34: 449-462.

Nakashima, Y. and Kamiya, S., 2007. Mathematica programs for the analysis of three-dimensional pore connectivity and anisotropic tortuosity of porous rocks using X-ray computed tomography image data. Journal of Nuclear Science and Technology, 44(9): 1233-1247.

Ohgaki, T. et al., 2006. In-situ high-resolution X-ray CT observation of compressive and damage behaviour of aluminium foams by local Tomography Technique. Advanced Engineering Materials, 8(6): 473-475.

Pone, J.D.N., Hile, L.M., Halleck, P.M. and Mathews, J.P., In prep. Three-dimensional carbon dioxide-induced strain distributions within a confined bituminous coal. International Journal of Coal Geology.

Raynaud, S., Fabre, D., Mazerolle, F., Geraud, Y. and Latiere, H.J., 1989. Analysis of the Internal Structure of Rocks and Characterization of Mechanical Deformation by a Non-Destructive Method - X-Ray Tomodensitometry. Tectonophysics, 159(1-2): 149-159.

Ren, J. and Ge, X., 2004. Computerized tomography examination of damage tests on rocks under triaxial compression. Rock Mechanics and Rock Engineering, 37(1): 83-93.

Reucroft, P.J., 1987. Effect of pressure on carbon dioxide induced coal swelling. Fuel, 1: 72-75.

Reucroft, P.J. and Patel, H., 1986. Gas-induced swelling in coal. Fuel, 65(6): 816-820.

Robertson, E.P. and Christiansen, R.L., 2005. Modeling permeability in coal using sorption-induced strain data. SPE, 97068.

Scott, A.C., 2002. Coal petrology and the origin of coal macerals: A way ahead? International Journal of Coal Geology, 50(1-4): 119-134.

Seidle, J.P. and Huitt, L.G., 1995. Experimental measurement of coal matrix shrinkage due to gas desorption and implications for cleat permeability increases. Society of Petroleum Engineers, SPE30010: 575-582.

Smith, T.S. and Bay, B.K., 2001. Experimental measurement of strains using digital volume correlation. In: G.F. Lucas, Mckeighan, P.C., Ransom, J.S. (Editor), Nontraditional methods of sensing stress, strain, and damage in material and structures: Second volume. American Society for Testing and Materials, ASTM STP 1323, West Conshohocken, PA, 2001.

Smith, T.S., Bay, B.K. and Rashid, M.M., 2002. Digital volume correlation including rotational degrees of freedom during minimization. Experimental Mechanics, 42(3): 272-278.

Toda, H., Kobayashi, M., Uesugi, K., Wilkinson, D.S. and Kobayashi, T., 2007. 3D strain mapping inside materials by microstructural tracking in tomographic volumes In: A.A. Mammoli (Editor), Computational Methods and Experiments in Materials Characterisation III, New Mexico, USA, pp. 176-186.

Vacher, P., Dumoulin, S., Morestin, F. and Mguil-Touchal, S., 1999. Bidimensional strain measurement using digital images. Proceedings of the Institution of Mechanical Engineers Part C-Journal of Mechanical Engineering Science, 213(8): 811-817.

Van Geet, M. and Swennen, R., 2001. Quantitative 3D-fracture analysis by means of microfocus X-ray computer tomography (μCT): an example from coal. Geophysical Research Letters, 28(17): 3333-3336.

Van Geet, M., Swennen, R. and Wevers, M., 2000. Quantitative analysis of reservoir rocks by microfocus X-ray computerised tomography. Sedimentary Geology, 132(1-2): 25-36.

Verhulp, E., van Rietbergen, B. and Huiskes, R., 2004. A three-dimensional digital image correlation technique for strain measurements in microstructures. Journal of Biomechanics, 37(9): 1313-1320.

Viete, D.R. and Ranjith, P.G., 2006. The effect of CO_2 on the geomechanical and permeability behaviour of brown coal: Implications for coal seam CO_2 sequestration. International Journal of Coal Geology, 66(3): 204-216.

Vukadin, V., 2007. Modeling of the stress-strain behavior in hard soils and soft rocks. Acta Geotechnica Slovenica, 4(2): 4-15.

Walker, P.L., 1981. Microporosity in coal: its characterization and its implications for coal utilization. Phylosophical Transactions of the Royal Society of London. Series A, Mathematical and Physical Sciences, 300(1453): 65-81.

Walker, P.L., Jr., Verma, S.K., Rivera-Utrilla, J. and Davis, A., 1988a. Densities, porosities and surface areas of coal macerals as measured by their interaction with gases, vapours and liquids. Fuel, 67(12): 1615-1623.

Walker, P.L., Jr., Verma, S.K., Rivera-Utrilla, J. and Rashid Khan, M., 1988b. Direct measurement of expansion in coals and marcerals induced by carbon dioxide and methanol. Fuel, 67(5): 719-726.

Walker, P.L. and Mahajan, O.P., 1993. Pore structure in coals. Energy & Fuels, 7(4): 559-560.

Wang, F.Y., Zhu P, Z.H. and Rudolph, M.V., 2007. Mass transfer in coal seams for CO_2 sequestration. AIChE Journal, 53(4): 1028-1049.

White, C.M. et al., 2005. Sequestration of carbon dioxide in coal with enhanced coalbed methane recovery - A review. Energy and Fuels, 19(3): 659-724.

Zienkiewicz, O.C. and Taylor, R.L., 1989. The finite element method, 1. McGraw-Hill Book Company, London, 616 pp.

Zutshi, A. and Harpalani, S., 2004. Matrix swelling with CO_2 injection in a CBM reservoir and its impact on permeability of coal, International Coalbed Methane Symposium, University of Alabama, Tuscaloosa.

Chapter 3

Sorption and Kinetics of Carbon Dioxide and Methane in Confined and Unconfined Bituminous Coal.

Abstract

Carbon dioxide injection into coal formations provides opportunity to sequester carbon while simultaneously enhancing methane recovery. Although powdered coal sample provide a quick indication of the gas sorption capacity and kinetics, underground storage take place within compact coal monoliths and therefore it is necessary to account for in-situ conditions impacts for meaningful estimates. This study presents the sorption rates and the sorption capacities of carbon dioxide and methane, and analyzes the kinetics of the complex, heterogeneous processes occurring in a bituminous coal samples while confined to simulate the in-situ stress conditions. The impact of confining stress on the sorption capacity was evaluated. The application of 6.9 and 13.8 MPa of confining stress (equivalent depth of 1000 and 2000 feet) contributed to 39% and 64% of CO_2 sorption capacity reduction respectively compare to values obtained from a powder sample. Similarly, 85% and 91% CH_4 uptake capacity reduction was observed at the same confining stress values. The time-dependent gases diffusion parameters were quantified using the volumetric method with a mathematical analysis of the pressure-decay data. Results emphasize that gas sorption and transport in coal matrix is interplay of flow, molecular or surface diffusion processes simultaneously taking place in the macropores

and micropores, respectively. It is found that the overall gas movement is hindered by confining stresses and takes place at rates significantly less than that in the macropores.

Introduction

The prospect of injecting carbon dioxide into coalbed reservoirs for sequestration and enhanced coalbed methane recovery (CBM/ECBM) purposes is one of the climate change mitigation options. Available evidence suggests that globally, there is a technical potential of about 2,000 $GtCO_2$ of storage capacity in geological formations, with at least 15 $GtCO_2$ in unmineable coal formations (IPCC, 2005). Considering that ECBM could make a substantial cut into greenhouse gas emissions, policy makers and potential investors around the world are in needs of reliable estimates of storage capacities and an indication of long term sustainability. Valuable resources and time could be wasted if sorption capacities are made based on unreliable data (Bradshaw et al., 2007). Injection into coal formations provides unique advantage over other potential geological storage options with the possibility to sequester carbon while simultaneously enhancing methane recovery. The characterization of sorption capacity and transport of gases in coal is required for the successful implementation. In spite of extensive research, there are still gaps in our fundamental understanding about aspects of coal interactions with CO_2 (Majewska and Zietek, 2007). Among these are the sorption capacities and the kinetics of carbon dioxide and methane transport through the coal structure at in-situ stress conditions. The heterogeneous nature of coal introduces a number of complex factors into

various processes involved in the retention of gas, its release and subsequent flow through the coal seam.

Gas uptake capacity and transport rates estimation rely on simple calculations. However, the interplay of different in-situ processes and conditions makes the evaluation tedious. Existing CO_2 storage capacity estimates are highly scattered and sometimes contradictory (Goodman et al., 2004; Yu et al., 2008). Some of the inconsistencies are consequences of using inappropriate methodology to derive rough estimates or due to the desire to make quick assessments with limited or no data as noted Bradshaw et al. (2007). Although crushed coal provides useful information for coal structure characterization, underground storage take place within compact coal monoliths. There are evidences that in-situ stress conditions affects coal uptake capacity (Hile, 2006; Smith et al., 2007), influence strain distribution (Pone et al., 2008) and consequently impacts gas movement in coal.

Characterization of coal structure and behavior and appropriate interpretation of laboratory experimental results are prerequisite for the generation of reliable estimates of CO_2 and CH_4 sorption capacities and diffusion rates in coal. This paper focuses on the characterization of coal-gas system dynamic behavior during carbon dioxide and methane sorption at replicated in-situ confining stress conditions. Effect of confining stress on sorption capacity and the evaluation of gases transport rates and its variation with time in coal at constant effective stress is evaluated. The rank of the coal, the temperature and the confining stresses used in this work are consistent with potential ECBM sites. The relationship between sorption rates of methane and carbon dioxide and the effective stress is discussed and evaluated with a descriptive mathematical model developed based on

experimental data. Fractures, cleats, macropores and micropores networks of coal behave differently from Darcy flow. Information collected from the same coal, but unconfined and crushed at -60 mesh allows comparison. Availability of reliable data is crucial for the development and management of coal seams sequestration and enhanced methane recovery projects. Sorption and transport rates obtained can be used in reservoirs simulators of enhanced coalbed methane recovery and carbon dioxide sequestration in unmineable coal seams.

Background

Sorption and diffusivity are primary characteristics required for any meaningful evaluation and predictive modeling of coal reservoirs (Saghafi et al., 2007). Physically, coal is viewed as a heterogeneous porous medium consisting of bulk matrix system of low porosity and low permeability surrounded by a system of fractures of high permeability and high porosity. The bulk matrix of coal is known to consist of a system of micropores on the order of 5 to 10 $\dot{A}$ in diameter while the cleats and fractures system is characterized by pores ranging from micropores dimensions to several microns in size (Van Krevelen, 1993). Cleats with size varying from micrometer to several centimeters have also been reported (McCulloch et al., 1974) and the cleat frequency depended on the rank and geologic history of the coal. The microporous texture of coal accounts for the observed high CO_2 determined surface area ranging from 200 to 300 m^2/g (Marsh, 1965) and contributes depending on experimental conditions, rank and physical characteristics of coal to more than 95% of the gas uptake capacity (Shi and Durucan, 2005). The

permeability of the coal seam is highly influenced by fracture and cleats size and distribution (Karn et al., 1975; Karn et al., 1970).

Gas Sorption in Coal

The complexity of coal structure due to the mixture of organic and inorganic matter has made fundamental sorption studies on coal an ongoing investigation over the years (Airey, 1968; Bertard et al., 1970; Harpalani et al., 2006; Vinokurova, 1978). Although coal structure presents challenging scientific questions, the general understanding however is clear (Berkowits, 1985). Interaction of coal structure with some gases and liquids leads to a chain of physical and chemical reactions. Among these are adsorption, absorption, persorption, and chemisorption. All these processes are generally designated through the literature as sorption without distinction. Different conditions, such as pressure, temperature, physical nature of the coal and sorbate influence the extent to which each of these events can occur. Additional factors affecting the sorption characteristics of coal are the presence of pores with highly polar surfaces and its non-rigid structure when exposed to certain adsorbates (Mahajan, 1991).

One of the main characteristic deserving attentions is structure change during sorption processes because of its impact on porosity and hence capacity. These variations have a strong influence on the subsequent amount and the kinetics of gas uptake or desorbed from coal. The swelling behavior of coal cross-linked macromolecular network when exposed to certain gases or liquid sorbates has been observed in several investigations. This subject is critically reviewed by Given et al. (1986) and others

(Ceglarska-Stefanska and Czaplinski, 1993; Czaplinski, 1986a; Czaplinski, 1986b; Czaplinski, 1986c; Goodman et al., 2005; Gorucu et al., 2005; Hall et al., 1988; Larsen, 2004; Nelson et al., 1980a; Nelson et al., 1980b; Nishioka, 1993a; Nishioka, 1993b; Reucroft and Patel, 1986; Reucroft and Patel, 1983; Sethuraman and Reucroft, 1987; Strezov et al., 2005). However, swelling data characterizing coal under stress are limited. Compression/compaction as well as regional swelling is expected from coal structure under stresses (Pone et al., 2008). More studies of coal under stress are required to understand the real behavior of coal during CO_2 sequestration or methane recovery.

In a key contribution describing a novel technique for the removal of methane from coal, Every and Dell'osso (1972) proved that under laboratory conditions, it was possible to displace 90% of the residual methane from crushed coal at ambient temperature within one week by carbon dioxide sorption. They also showed that CO_2 had high affinity with coal structure, displacing 3 times more methane than air and 5 times more than helium, as demonstrated earlier by Graham (1919). These two observations are some of the earliest investigation of the industrial enhanced methane recovery and later CO_2 sequestration in coal seam.

Gas Transport in Coal

Investigation of gases sorption kinetics in coal structure is of great importance (Walker et al., 1966). The movement of gas in coal pores network occurs as a result of both pressure and concentration gradients (Gilman and Beckie, 2000). It can also be explained by the energy fluctuation due to the sorption processes. The mechanism of gas

transport maybe molecular diffusion through the micropores, bulk diffusion through the macro/mesopores, or permeation through the fracture system of the coalbed (Shi and Durucan, 2005). Transport of gas in coalbeds takes place in a multiscale system, often characterized by a distinctive matrix structure involving a simplified bimodal pore size distribution (Yi et al., 2007). The interplay of the high-flow rate of the macroscopic fracture network and the low-flow rate of the matrix during adsorption or desorption in coals needs to be well characterized to allow management of injection and production processes. Existing models used for coalbed simulators assume gas sorption, or desorption, is being controlled by a constant diffusivity coefficient from spherical objects or "matchsticks" sets connected by a relatively large fracture network (King and Ertekin, 1989). Application of this general model may results in the introduction of large errors in the estimation of sorption capacity and the prediction of flow behavior. Rigorous predictive model should encompass all forms of gas transport mechanisms.

The process of gas injection and production from coal seam faces number of challenges (Reeves et al., 2008). The evaluation of sorption and transport of gas in coal is been less successful using analytical approaches developed for conventional reservoir characterization. A recent study compared the accuracy of three popular field-permeability models when applied to laboratory-generated, sorption-affected permeability data and found poor agreement (Robertson and Christiansen, 2005). Much of this has to do with the complex structure of coal that has a multi-scale of pore structure varying from nanometer to micrometer size (Gamson et al., 1993). Furthermore, many CBM/ECBM reservoir simulators operate with a single-step unipore diffusion model (Busch et al., 2004) which although a useful approximation, is a simplistic representation

of transport process in coal. This is further complicated by various sorption types and mechanisms that can occur, the different time frames over which sorption becomes effective, and the different physical states in which the CO_2 might occur (Bradshaw et al., 2007). Many of the discrepancies between the various sorption rates reported can be attributed to the dynamic pore structure variation and different diffusion lengths (Olague and Smith, 1989).

As fluid flows through a structure of micro to a nanometer size, the effect of interaction between the fluid molecules and the solid wall molecules is much more significant than in its bulk case. Usually, the fluid-wall interaction will induce a strong heterogeneity in the fluid, featured with the layered fluid molecules adjacent to the solid wall, and strong fluctuations in the fluid density in the near-wall region. Owing to this heterogeneity, the equilibrium and dynamic behaviors of the fluid may become significantly different from those at the macroscopic scale. Under such circumstances, the conventional hydrodynamic models, e.g., the Navier-Stokes equations will become invalid since the heterogeneity is usually neglected in these models. Therefore, one must resort to more elaborate models into which the microscopic interactions are incorporated appropriately to study these small scale flows.

A descriptive model of gas movement in coal structure based on experimental data was developed. This paper focuses primarily on the characterization of coal-gas system dynamic behavior during carbon dioxide and methane sorption at replicated stress and temperature encountered in-situ. The effect of confining stress on sorption capacity and the evaluation of gases transport rates and its variation with time in coal at constant effective stress was quantify. The relationship between sorption rates of methane and

carbon dioxide and the effective stress is discussed and evaluated with the model. Information collected from the same coal, but unconfined and crushed at -60 mesh allowed comparison. Availability of reliable data is crucial for the development and management of coal seams sequestration and enhanced methane recovery projects. Sorption and transport rates obtained can be used in reservoirs simulators of enhanced coalbed methane recovery and carbon dioxide sequestration in unmineable coal seams.

Although crushed coal provides useful information for coal structure characterization, underground gas storage and desorption take place within compact coal monoliths. The pulverization of coal contribute to the mixture and dispersion of all different lithotypes and microlithotypes so that measured results of properties describe average values statistically, which do not resemble the property of a distinct macro-structural unit (Mathews et al., 2001). Therefore, transfer of properties obtained from crushed unconfined coal samples to solid coal is not justified. Powder and whole coal samples were used for this study.

Experimental Procedures

Samples Preparation

Coal samples used for this study were prepared from a single block collected from the Hazard No. 9 coal seam, Perry County of the Western Kentucky Coalfield. The highwall overburden, mostly sandstone was estimated to be 200 m thick and the seam to be 2 m thick. The block was removed and coated with water-based polycrylic protective

finish to prevent any further oxidation and dehydration of the sample. It was cast in plaster to aid the coring process. Multiple side-by-side cores were obtained parallel to the bedding plane. The cores were preserved in sealed container under nitrogen environment. The end surfaces of the cores were polished to produce a flat and parallel surface for the application of uniform stress and gas distribution.

Core samples of 2.5 cm (1 inch) in diameter and 6.3 cm (2.5 inches) average length were hydraulically confined to replicate the in-situ conditions during sorption experiments. Some of the cores obtained were cut using diamond saw to produce (~2 cm x 1cm x 1cm) rectangular shape samples used for sorption measurements under zero-confining stress. The remaining pieces were crushed at < 200 microns particles (60 - 80 mesh) size and used for sorption measurements on powder samples. Proximate and Ultimate analyses of the sample were determined.

Isotherm Measurement Method

Core samples were evacuated for 48 h and powder samples for 24 h to remove any residual gases and weakly-bond water molecules before the measurements were performed. The gas accessible void volume in the sample cell was estimated using helium displacement. Measurements were made using the volumetric gas adsorption apparatus shown schematically in Figure 3-1. Briefly, the system consisted of a sample cell and a reference cell, both of which have accurately known volumes determined by Boyle's law. All cells are contained in a temperature controlled environment (±0.1 °C). Two distinct system configurations were designed to accommodate measurements under stress and

without stress. A Temco® designed pressure vessel was used for measurements under stress while a customized high pressure chamber was used for measurements at zero-confining stress. The apparatus consisted of a reference cell of approximately 10 ml and a sample cell of about 3 ml.

After removing the helium under vacuum, the reference cell was pressurized with CH_4 or CO_2. After the thermal equilibrium is achieved, a portion of the gas (CH_4 or CO_2) was transferred from the reference cell into the sample cell. Pressure and temperature were monitored in both cells using high-precision pressure transducers. Sorption was rapid for the powdered coals, but long equilibration times were allowed for solid cores of coal. A few hours were sufficient for the sorption on powdered coal samples to establish a trend. At an arbitrary equilibrium point, the amounts of gas within both the reference and sample cell were calculated using the real gas law and the Span and Wagner values for the gas compressibility factor (Span and Wagner, 1996a). From the mass balance, the difference between the moles of gas transferred from the reference cell and the moles of gas calculated to be present in the He-estimated free-gas phase in the sample cell was considered to be the Gibbs excess adsorption. The reference cell was then pressurized with additional gas and the process was repeated. The incremental Gibbs excess adsorption (Δn_i^{ex}) at the end of i^{th} step is determined from equation 1 (Yu et al., 2008):

$$\Delta n_i^{ex} = \left(\frac{1}{RTm}\right)\left(V_R\left(\frac{P_{R,I}^i}{Z_{R,I}^i} - \frac{P_{R,F}^i}{Z_{R,F}^i}\right) - V_0\left(\frac{P_{S,Eq}^i}{Z_{S,Eq}^i} - \frac{P_{S,Eq}^{i-1}}{Z_{S,Eq}^{i-1}}\right)\right) \quad (1)$$

where the subscripts, $I, F,$ and Eq, refer to the initial conditions in the cell, final gas expansion, and adsorption apparent equilibrium or steady state; the subscripts, R and

S represent the reference and sample cell; the superscripts, i and $(i-1)$ represent the i^{th} and $(i-1)^{th}$ step, respectively; and P is the pressure, Z is the compressibility factor of the gas, T is the temperature, R is the molar gas constant, m is the mass of the coal sample, V_R and V_0 are the volume of the reference cell and the void volume in the sample cell, respectively.

Measurements were performed in small time increments as long as the gas sorption volumes are large, but these increments were lengthened as the sorbed volume decreases. The gas volume readings were continued for several days until the volume change becomes too small to measure. Gas injection pressure was kept constant around 3.1 MPa (450 psi) for all sorption cycles. Confining stress of 6.9 MPa (1000 psi) and 13.8 MPa (2000 psi) were used during measurements. Adsorption isotherms were plotted as the total amount of excess adsorbed gas versus elapsed time steps. An error analysis similar to that reported by (Ozdemir, 2004) indicated that the error associated with each data point could be as high as 2%. A detail mathematical description of the volumetric method is provided by Mavor et al. (1990) and Odzemir et al. (2003).

Mathematical Modeling of Sorption Kinetics

Sorption kinetic data was obtained by monitoring the rate of pressure equilibration during individual steps of volumetric sorption experiments. Pressure decays data were used to compute diffusion coefficients. For diffusion in a system such as that used in the present work, the differential equation as written by Fourier (1822) or commonly known as Fick's second law

$$\frac{\partial C}{\partial t} = \frac{1}{r}\frac{\partial}{\partial r}\left(rD\frac{\partial C}{\partial r}\right) \quad (2)$$

with boundary conditions

$$C = 0 \; at \; t = 0 \quad (3)$$

will hold, provided that diffusion occurs primarily in the radial direction. Assuming also that there were no angular concentration gradients, and that the diffusion coefficient was isotropic and independent of concentration at the gas concentration used. In equations 2 and 3, C is concentration, t is time, r is the radial distance, and D is the diffusion coefficient.

Fourier (1822), Carman and Haul (1954) and later Crank (1975) solved the above diffusivity equations for the case where diffusion occurs from a solution of limited volume, i.e., when the concentration of gas or the total amount of gas is changing at the surface of the sample. The solution was written in more convenient form by Carman and Haul (1954) as

$$1 - \frac{M_t}{M_\infty} = \sum_{n=1}^{\infty} \frac{4\alpha(1+\alpha)}{4+4\alpha+\alpha^2 q_n^2} \exp\left(\frac{-q_n^2 Dt}{a^2}\right) \quad (4)$$

where M_t is the total amount of gas sorbed after time t, M_∞ is the amount after infinite time and q_n are the non-zero roots of the equation:

$$\alpha q_n J_0(q_n) + 2J_1(q_n) = 0 \quad (5)$$

where J_n are Bessel function of n^{th} order.

In Crank's solution, the diffusivity equations reflect a condition in which the total amount of gas in a limited volume is changing at the surface of the sample. When the sorbate is a pure gas, the concentration is measured by the pressure, p, i.e. the initial pressure is p_1, the pressure at $t = 0$ is p_2 and at $t = \infty$ it is p_∞. It is then follows that

$$1 - \frac{M_t}{M_\infty} = \frac{p - p_\infty}{p_2 - p_\infty}, \tag{6}$$

$$\alpha = \frac{p_\infty - p_1}{p_2 - p_\infty}. \tag{7}$$

This method is particularly well suited for gases diffusion estimation, since measurement of a sorption isotherm by the volumetric method is normally carried out in steps. The p_∞ attained in one step becomes p_1 for the next.

The six roots of q_n for different values of α are given by Crank (1975) to assist the evaluation of equation 5. The convergence of the series in equation 4 becomes inconveniently slow for numerical evaluation when Dt/r^2 is small. An alternative solution was proposed by Carman and Haul (1954) which is accurate up to considerably higher values of M_t/M_∞. Considering the non-ideality of the gas, the pressure values were corrected using the compressibility factor (Span and Wagner, 1996b) and the Carman and Haul (1954) rewritten as follows:

$$\frac{p/z - p_\infty/z_\infty}{p_2/z_2 - p_\infty/z_\infty} =$$

$$\frac{\gamma_3}{\gamma_3+\gamma_4} \exp\{4\gamma_3^2 Dt/(a^2\alpha^2)\} \operatorname{erfc}\left\{\frac{2\gamma_3}{\alpha}\left(\frac{Dt}{a^2}\right)^{1/2}\right\} +$$

$$\frac{\gamma_4}{\gamma_3+\gamma_4} \exp\{4\gamma_4^2 Dt/(a^2\alpha^2)\} \operatorname{erfc}\left\{-\frac{2\gamma_4}{\alpha}\left(\frac{Dt}{a^2}\right)^{1/2}\right\} \tag{8}$$

where

$$\gamma_3 = \frac{1}{2}\left\{(1+\alpha)^{1/2} + 1\right\}, \qquad \gamma_4 = \gamma_3 - 1 \tag{9}$$

Effective diffusivity (D/a^2) values were calculated from the experimental pressure-time data using equation 6-9 as follows. The raw pressure decay data were corrected for the non-ideality of the gas using the compressibility factor from Span and

Wagner (1996). From the knowledge of the initial and final pressure values, α was established. Then, a model pressure-decay curve was generated. Experimental M_t/M_∞ values were then plotted against time t and compared to the predicted M_t/M_∞ versus time generated by applying an estimated diffusivity value. The least deviation from the experimental M_t/M_∞ versus time curve was obtained through iterative method in fitting the best diffusivity value. Finally, a value of diffusivity was chosen which gave the best fit of the model pressure-decay curve with the experimental pressure-decay curve, in the same manner as Durrill and Griskey (1966) , Singh et al. (1996), Chen and Rizvi (2006) and Li et al. (2006).

Results and Discussion

Sorption Capacity

The sorption of gases as a function of time t was obtained on the basis of the difference between the initial amount of gas introduced into the cell and the amount of the gas remaining in the dead space of the cell at any given time t_i from $t = 0\ to\ t_{eq}$ (equilibrium) as shown in equation 1. The pressure decrease in the system was measured automatically and allowed simultaneous monitoring and recording of time and pressure. The injection pressure was 3.1 MPa in all the sorption cycles. Capacities values reported were not corrected for mineral matter content.

Figure 3-2 shows the uptake of CO_2 and CH_4 on a powdered sample for short ($t \leq$ 0.1 day) and long ($t \rightarrow eq$) coal-gas contact times at 20°C. It can be seen that the sorption of CO_2 occurred rapidly, achieving more than 95% of the total capacity during the first few hours of the experiment. The sorption of CH_4 occurred relatively slowly, achieving almost 75% of the total capacity at the same period. Figure 3-2 and 3-3 shows that CO_2 had higher affinity with coal structure. Similar sorption studies on powder coal have proved that CO_2 behaves preferentially in sorption as compared with CH_4. Cui et al. (2004) indicated that due to its relatively smaller kinetic diameter, CO_2 can permeate not only macropores but also ultra micropores. According to Mastalerz et al. (2004), this difference in the sorption of CO_2 and CH_4 is justified by the fact that adsorption into the micropores is the major mechanism for CH_4, whereas both adsorption into the micropores and absorption into organic matrix of coal is dominant for CO_2. Milewska-Duda et al. (2000) based on modeling data suggested that for CO_2, the contribution of pure absorption is comparable to that of pure adsorption, whereas for CH_4 the pure absorption is much lower. Reucroft (1987) stated that CO_2 dissolution into coal organic structure of coal contributed up to half of the total uptake. Although the dominant mechanism between adsorption and absorption still to be quantified, it is clear that for sequestration of CO_2 in coal seams, attention must be paid to the possible effects of dissolved CO_2 on the structure and its impacts of the coal behavior as suggested by Larsen (2004).

The results depicted in Figure 3-5 show that the uptake of CO_2 and CH_4 varies with the physical state of the sample. Specifically the uptake decreased with increasing stress condition. The data shown in Figures 3-3 and 3-4 indicate the sorption capacity

achieved values of about 1.2, 1.4, 0.9, and 0.5 $mmole_{CO2}/g_{coal}$ for powder, non-powder unconfined, confined at 6.9MPa and confined at 13.8 MPa respectively for CO_2. Similarly with CH_4, we observed a sorption capacity of about 0.7, 0.6, 0.1 and 0.06 $mmole_{CH4}/g_{coal}$ for powder, non-powder unconfined, confined at 6.9MPa and confined at 13.8 MPa respectively. The sorption process under confining stress was very slow in comparison to powdered coal. Non-powder unconfined coal sample sorbed more CO_2 compare to powder sample. This may be an indication that the coal pulverization contributed to the dissolution of the synergistic effects of coal marcerals as noted early. Sorption studies of CO_2 and CH_4 on non-powder confined coal samples are limited. Hile (2006) analyzing the impacts of confining stress on the CO_2 uptake capacity of Pittsburgh # 8 coal reported 80% decreases compare to crushed coal. These results were duplicated by Jikich et al. (2007). Studying the sorption of CO_2 on non-powder unconfined coal samples, Smith et al. (2007) and Kelemen (2007) also reported a sorption capacity reduction. These results indicate that the diffusion of CO_2 molecules through coal multi-scale pores was the rate-controlling process in the sorption of this gas.

Results for powdered and non-powdered coal sample were of interest to evaluate the influence of grinding and stresses on the sorption kinetic and capacity of these gases. The results obtained could be useful for establishing the suitable data for reservoirs simulation and the prediction of CO_2 storage capacity in coal seams.

Sorption Kinetics

The uptake of organic molecules, methane and carbon dioxide, into coal structure may be accompanied by the physical softening of the structure which induced compression/compaction and swelling of the coal matrix. Non-uniform swelling in turn gives rises to differential stresses and the visco-elastic response of the structure to these stresses may exert a critical influence on the transport within coal's matrix. The resulting kinetics of penetration may vary widely and their interpretation requires information obtained on the particular coal-gas system. Figures 3-6 and 3-7 show the variation of diffusivity constant as a function of time for CO_2 and CH_4 respectively. Additionally, there are illustrating the impacts of physical state of the samples on the diffusion processes. Diffusivities constant for CO_2 and CH_4 decrease with time. Initial and final values of diffusivity coefficient for both CO_2 and CH_4 are reported in Table 2. The early stage of the transport of gas in coal is dominated by Darcy's type flow and depending on the stress state of the sample the process becomes diffusion controlled later. It is clear that diffusion plays a major part into the CO_2 uptake compare to CH_4. This observation confirms that CO_2 transport in coal micro and nanopores is dominated by Knudsen, surface or molecular diffusion. Different gas sorption rates corresponding to different stages of the experiment are evident in Figure 3-6 and 3-7. This process is also influenced by the interaction of CO_2 with coal pores network. It is important to note that all these processes overlap. Hence, a constant diffusion coefficient might not be accurate for CO_2 transport characterization in non-powder confined coals. Figure 3-8 described the contrast between CO_2 and CH_4 sorption rates in coal core at 6.9 MPa confining stress.

This figure shows clearly that the imbibitions and dissolution of CO_2 in coal matrix which has been reported previously leads to a different transport behavior of CH_4 and CO_2 in coal.

Data extracted from Figures 3-2 to 3-8, suggests that gas uptake and the presence of confining stress influence the coal-gas system in twofold. The sorption of gas leads to a non-uniform deformation of the coal matrix, which consequently impact the pore volume of the coal matrix. As results, a substantial uptake reduction was noted. Secondly, although the effects of macropore's volume change due to stresses on the overall gas uptake may be negligible, their promoted a considerable retardation effect on flow and diffusion in the matrix.

Conclusions

Gas sorption and transport behavior in powder and non-powder confined coal sample was quantified for CO_2 gas uptake capacity. A method based on pressure-decay was adapted to characterize the transport behavior of CH_4 and CO_2 in coal. The sorption capacity and the kinetics of gas in coal are both influenced by the stress state of the sample. The application of 6.9 and 13.8 MPa of confining stress contributed to 39% and 64% of CO_2 sorption capacity reductions respectively in comparison to powder coal. Similarly, 85% and 91% CH_4 uptake capacity reductions due to 6.9 and 13.8 MPa of confining stress in comparison to powder coal were recorded. The diffusion of CH_4 and CO_2 in confined coal is described with varying diffusivity coefficients dynamically throughout the sorption process. This data questions the applicability of capacity estimates from

powdered coal and further demonstrates the importance of in-situ stress conditions. Investigation of sorption and diffusion of gases in coal at in-situ stress conditions are limited and should be investigated further.

References

Airey, E.M., 1968. Gas emission from broken coal . An experimental and theoretical investigation. International Journal of Rock Mechanics and Mining Sciences, 5(6): 475.

Berkowits, N., 1985. Coal science and technology 7- The chemistry of coal. Elsevier Science, London.

Bertard, C., Bruyet, B. and Gunther, J., 1970. Determination of desorbable gas concentration of coal (direct method). International Journal of Rock Mechanics and Mining Sciences, 7(1): 43-65.

Bradshaw, J. et al., 2007. CO_2 storage capacity estimation: Issues and development of standards. International Journal of Greenhouse Gas Control, 1(1): 62-68.

Busch, A., Gensterblum, Y., Krooss, B.M. and Littke, R., 2004. Methane and carbon dioxide adsorption-diffusion experiments on coal: upscaling and modeling. International Journal of Coal Geology, 60(2-4): 151-168.

Carman, P.C. and Haul, R.A.W., 1954. Measurement of diffusion coefficients. Proceedings of the Royal Society of London Series a-Mathematical and Physical Sciences, 222(1148): 109-118.

Ceglarska-Stefanska, G. and Czaplinski, A., 1993. Correlation between sorption and dilatometric processes in hard coals. Fuel, 72(3): 413-417.

Cranks, J., 1975. The mathematics of diffusion. Clarendon Press, Oxford.

Cui, X., Bustin, R.M. and Dipple, G., 2004. Selective transport of CO_2, CH_4, and N_2 in coals: Insights from modeling of experimental gas adsorption data. Fuel, 83(3): 293-303.

Czaplinski, A., 1986a. Investigation of adsorption, dilatometry and strength of low rank coal. III. Investigations of simultaneous sorption together with expansion and desorption together with contraction kinetics of coal under the influence of carbon dioxide Archiwum Gornictwa, 31(3): 581-589.

Czaplinski, A., 1986b. Investigations of adsorption, dilatometry and strength of low rank coal. I. The apparatus and the method of simultaneous sorption and dilatometry measurements. Archiwum Gornictwa, 31(3): 563-568.

Czaplinski, A., 1986c. Investigations of adsorption, dilatometry and strength of low rank coal. IV. Investigations of simultaneous sorption together with expansion and desorption together with contraction kinetics of coal under influence of methane. Archiwum Gornictwa, 31(3): 591-598.

Durrill, P.L. and Griskey, R.G., 1966. Diffusion and solution of gases in thermally softened or molten polymers .I. Development of technique and determination of data. AIChE Journal, 12(6): 1147-1151.

Every, R.L. and Dell'osso, L.J., 1972. A new technique for the removal of methane from coal. Canadian Mining and Metallurgical Bulletin, 65(719): 143-150.

Fourier, J., 1822. The Analytical Theory of Heat. Dover, New York (1955).

Gamson, P.D., Beamish, B.B. and Johnson, D.P., 1993. Coal microstructure and micropermeability and their effects on natural gas recovery. Fuel, 72(1): 87-99.

Gilman, A. and Beckie, R., 2000. Flow of coal-bed methane to a gallery. Transport in Porous Media, 41(1): 1-16.

Goodman, A.L. et al., 2004. An inter-laboratory comparison of CO_2 isotherms measured on argonne premium coal samples. Energy Fuels, 18(4): 1175-1182.

Goodman, A.L., Favors, R.N., Hill, M.M. and Larsen, J.W., 2005. Structure changes in Pittsburgh no. 8 coal caused by sorption of CO_2 gas. Energy and Fuels, 19(4): 1759-1760.

Gorucu, F.B. et al., 2005. Matrix shrinkage and swelling effects on economics of enhanced coalbed methane production and CO_2 sequestration in coal. SPE Eastern Regional Meeting. Society of Petroleum Engineers, Richardson, TX 75083-3836, United States, Morgantown, West VA, United States, pp. 137-151.

Graham, I.J., 1919. The permeability of coal to gases. Transaction of the Institution of the Mining Engineers, 58(1): 32-38.

Hall, P.J., Marsh, H. and Thomas, K.M., 1988. Solvent induced swelling of coals to study macromolecular structure. Fuel, 67(6): 863-866.

Harpalani, S., Prusty, B.K. and Dutta, P., 2006. Methane/CO_2 sorption modeling for coalbed methane production and CO_2 Sequestration. Energy Fuels, 20(4): 1591-1599.

Hile, L.M., 2006. CO_2 sorption by Pittsburgh-seam coal subjected to confining pressure. Master Thesis, The Pennsylvania State University, University Park.

IPCC, 2005. Carbon Dioxide Capture and Storage: Special Report of the Intergovernmental Panel on Climate Change. Cambridge University Press.

Jikich, S.A., Mc Lendon, R., Seshadri, K., Irdi, G. and Smith, D.H., 2007. Carbon dioxide transport and sorption behavior in confined coal cores for enhanced coalbed methane and CO_2 sequestration, SPE Annual Technical Conference and Exhibition, Anaheim, CA, USA, 2007, SPE 109915

Karn, F.S., Friedel, R.A. and Sharkey, J.A.G., 1975. Mechanism of gas flow through coal. Fuel, 54(4): 279-282.

Karn, F.S., Friedel, R.A., Thames, B.M. and Sharkey, J.A.G., 1970. Gas transport through sections of solid coal. Fuel, 49(3): 249-256.

King, G.R. and Ertekin, T.M., 1989. A survey of mathematical models related to methane production from coal seams, International Coalbed Methane Symposium, University of Alabama, Tuscaloosa, Alabama, pp. 125–155.

Larsen, J.W., 2004. The effects of dissolved CO_2 on coal structure and properties. International Journal of Coal Geology, 57(1): 63-70.

Li, Z.W., Dong, M.Z., Li, S.L. and Dai, L.M., 2006. A new method for gas effective diffusion coefficient measurement in water-saturated porous rocks under high pressures. Journal of Porous Media, 9(5): 445-461.

Mahajan, O.P., 1991. CO_2 surface area of coals: The 25-year paradox. Carbon, 29(6): 735-742.

Majewska, Z. and Zietek, J., 2007. Changes of acoustic emission and strain in hard coal during gas sorption-desorption cycles. International Journal of Coal Geology, 70(4): 305-312.

Marsh, H., 1965. Determination of surface areas of coals - some physicochemical considerations. Fuel, 44(4): 253-260.

Mastalerz, M., Gluskoter, H. and Rupp, J., 2004. Carbon dioxide and methane sorption in high volatile bituminous coals from Indiana, USA. International Journal of Coal Geology, 60(1): 43-55.

Mathews, J.P., Karacan, O., Halleck, P., Mitchell, G.D. and Grader, A., 2001. Storage of pressurized carbon dioxide in coal observed using X-Ray tomography. First National Conference on Carbon Sequestration, 2001, Washington, DC, Online at: http://www.netl.doe.gov/publications/proceedings/01/carbon_seq/7a4.pdf.

Mavor, M.J., Owen, L.B. and Pratt, T.J., 1990. Measurement and evaluation of coal sorption isotherm data, 65th Annual Technical Conference and Exhibition of the Society of Petroleum Engineers, New Orleans, LA, USA, pp. SPE 20728.

McCulloch, C.M., Deul, M. and Jeran, P.W., 1974. Cleat in bituminous coalbeds, U.S. Bureau of Mines, Washington, DC.

Milewska-Duda, J., Duda, J., Nodzenski, A. and Lakatos, J., 2000. Absorption and adsorption of methane and carbon dioxide in hard coal and active carbon. Langmuir, 16(12): 5458-5466.

Nelson, J.R., Mahajan, O.P. and Walker, P.L., Jr., 1980a. Measurement of swelling of coals in organic liquids: a new approach. Fuel, 59(12): 831-837.

Nelson, J.R., Mahajan, O.P. and Walker, P.L., Jr., 1980b. Solvent induced swelling of coals. American Chemical Society, Division of Organic Coatings and Plastics Chemistry, Preprints, 43: 337-340.

Nishioka, M., 1993a. Dependence of solvent swelling on coal concentration. Fuel, 72(7): 1001-1005.

Nishioka, M., 1993b. Irreversibility of solvent swelling of bituminous coals. Fuel, 72(7): 997-1000.

Olague, N.E. and Smith, D.M., 1989. Diffusion of gases in American coals. Fuel, 68(11): 1381-1387.

Ozdemir, E., 2004. Chemistry of the adsorption of carbon dioxide by Argonne Premium coals and a model to simulate CO2 sequestration in coal seams, University of Pittsburgh, Pittsburgh, 321 pp.

Ozdemir, E., Morsi, B.I. and Schroeder, K., 2003. Importance of Volume Effects to Adsorption Isotherms of Carbon Dioxide on Coals. Langmuir, 19(23): 9764-9773.

Pone, J.D.N., Hile, L.M., Halleck, P.M. and Mathews, J.P., 2008. Three-dimensional carbon dioxide-induced strain distributions within a confined bituminous coal. International Journal of Coal Geology, doi:10.1016/j.coal.2008.08.003.

Reucroft, P.J., 1987. Effect of pressure on carbon dioxide induced coal swelling. Fuel, 1: 72-75.

Reucroft, P.J. and Patel, H., 1986. Gas-induced swelling in coal. Fuel, 65(6): 816-820.

Reucroft, P.J. and Patel, K.B., 1983. Surface area and swellability of coal. Fuel, 62(3): 279-284.

Robertson, E.P. and Christiansen, R.L., 2005. Modeling permeability in coal using sorption-induced strain data. SPE, 97068.

Saghafi, A., Faiz, M. and Roberts, D., 2007. CO_2 storage and gas diffusivity properties of coals from Sydney Basin, Australia. International Journal of Coal Geology, 70(1-3): 240-254.

Sethuraman, A.R. and Reucroft, P.J., 1987. Gas and vapor induced coal swelling, Prepr. Pap. Am. Chem. Soc., Div. Fuel Chem, Denver, CO, USA, pp. 259-264.

Shi, J.Q. and Durucan, S., 2005. CO_2 storage in deep unminable coal seams. Oil & Gas Science and Technology - Rev. IFP, 60(3): 547-558.

Singh, B., Rizvi, S.S.H. and Harriott, P., 1996. Measurement of diffusivity and solubility of carbon dioxide in gelatinized starch at elevated pressures. Industrial & Engineering Chemistry Research, 35(12): 4457-4463.

Smith, D.H., Jikich, S.A. and Seshadri, K., 2007. Carbon dioxide sorption isotherms and matrix transport rates for non-powdered coal, International Coalbed Methane Symposium, University of Alabama, AL, USA, May 21-25, 2007.

Span, R. and Wagner, W., 1996a. A new equation of state for carbon dioxide covering the fluid region from the triple-point temperature to 1100 K at pressures up to 800 MPa. Journal of Physical and Chemical Reference Data, 25(6): 1509-1596.

Span, R. and Wagner, W., 1996b. A new equation of state for carbon dioxide covering the fluid region from the triple-point temperature to 1100 K at pressures up to 800 MPa. Journal of Physical and Chemical Reference Data, 25: 1509-1596.

Strezov, V., Lucas, J.A. and Wall, T.F., 2005. Effect of pressure on the swelling of density separated coal particles. Fuel, 84(10): 1238-1245.

Van Krevelen, D.W., 1993. Coal: Topology - Physics - Chemistry - Constitution. 3rd edn. Elsevier, Amsterdam, 979 pp.

Vinokurova, E.B., 1978. The significance of sorption studies for practical coal mining. Khimiya Tverdogo Topliva, 12(6): 132-139.

Walker, P.L., Austin, L.G. and Nandi, S.P., 1966. Activated diffusion of gases in molecular-sieve materials. In: P.L. Walker (Editor), The Chemistry and Physics of Carbon. Marcel Dekker, New York, pp. 257-271.

Yi, J., Chongqing, U., Akkutlu, I.Y. and Deutsch, C.V., 2007. Gas sorption and transport in poroelastic coals, Society of Petroleum Engineers Rocky Mountain Oil & Gas Technology Symposium, Denver, Colorado, U.S.A.

Yu, H.G., Guo, W.J., Cheng, J.L. and Hu, Q.T., 2008. Impact of experimental parameters for manometric equipment on CO_2 isotherms measured: Comment on "Inter-laboratory comparison II: CO_2 isotherms measured on moisture-equilibrated Argonne premium coals at 55 degrees C and up to 15 MPa" by Goodman et al. (2007). International Journal of Coal Geology, 74(3-4): 250-258.

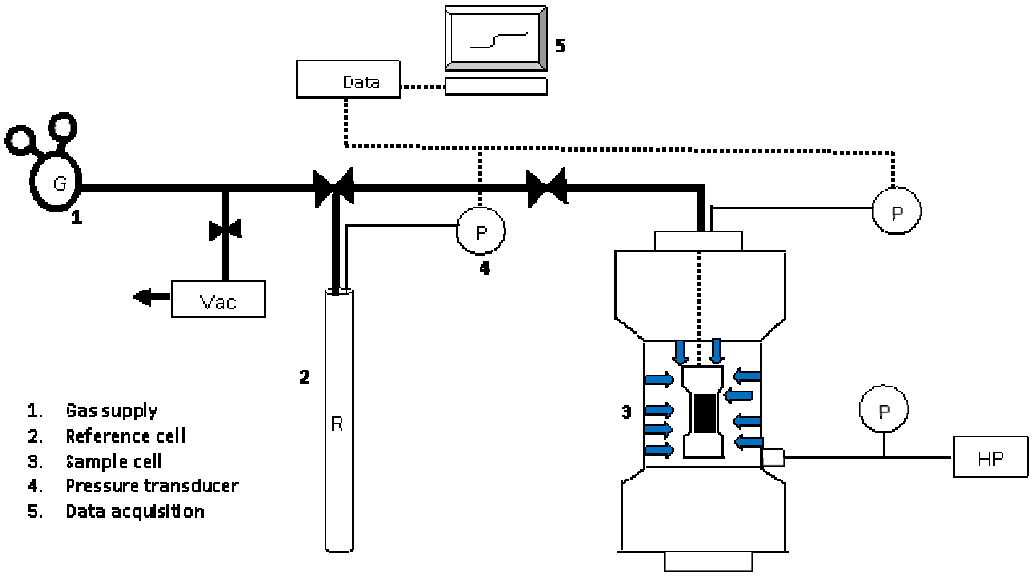

Figure 3-1: Experimental setup for the measurement of sorption and kinetics of gases in coal.

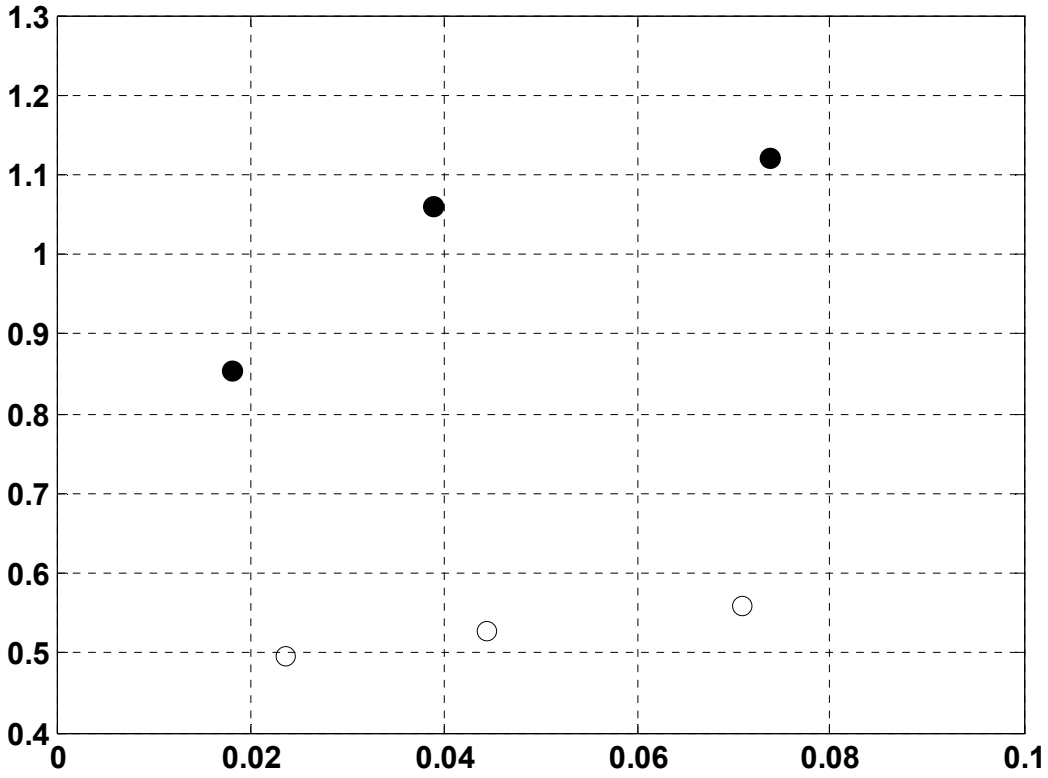

Figure 3-2: Methane (o) and carbon dioxide (•) excess sorption on powder (-60 mesh) coal at 20°C for short exposure time

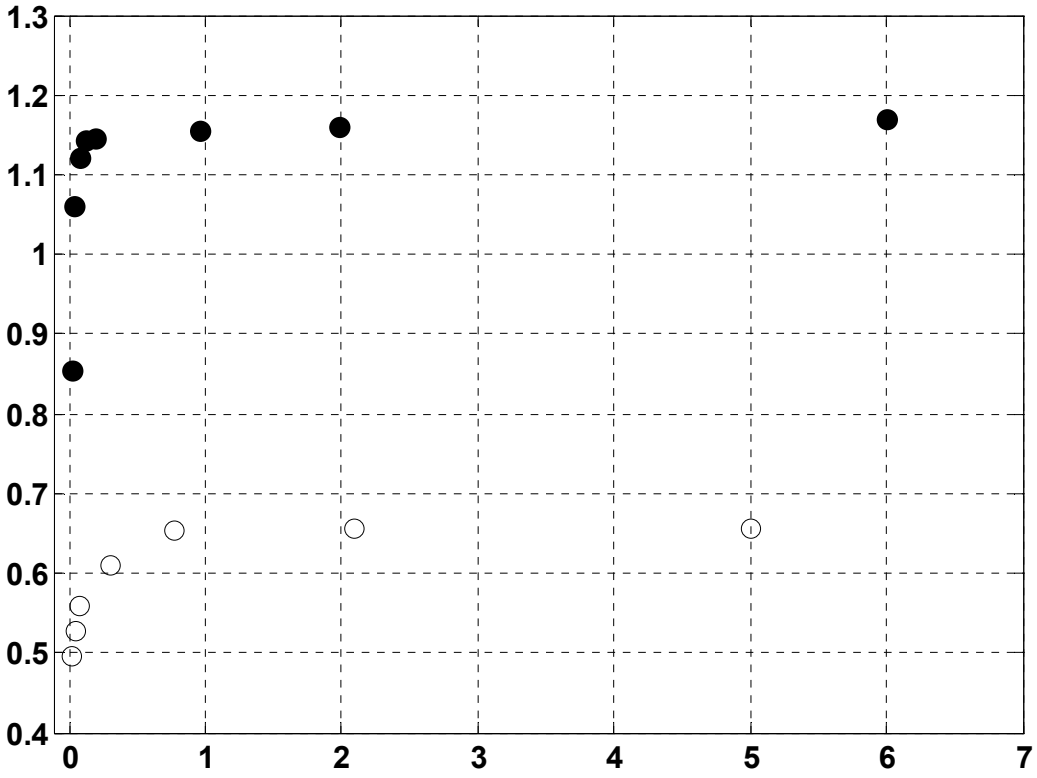

Figure 3-3: Methane (o) and carbon dioxide (•) excess sorption on powder (-60 mesh) coal at 20 °C for long exposure time

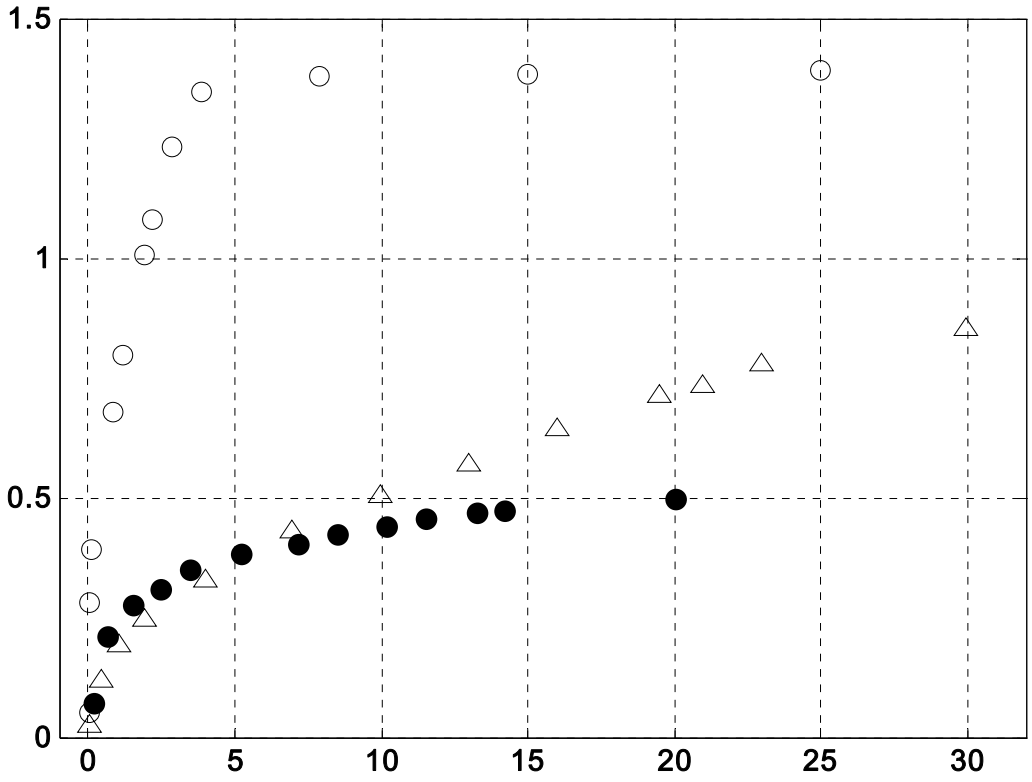

Figure 3-4: Carbon dioxide excess sorption on non-powder coal cores at 13.8 MPa (•), 6.9 MPa (Δ) confining stresses and non-powder unconfined (o).

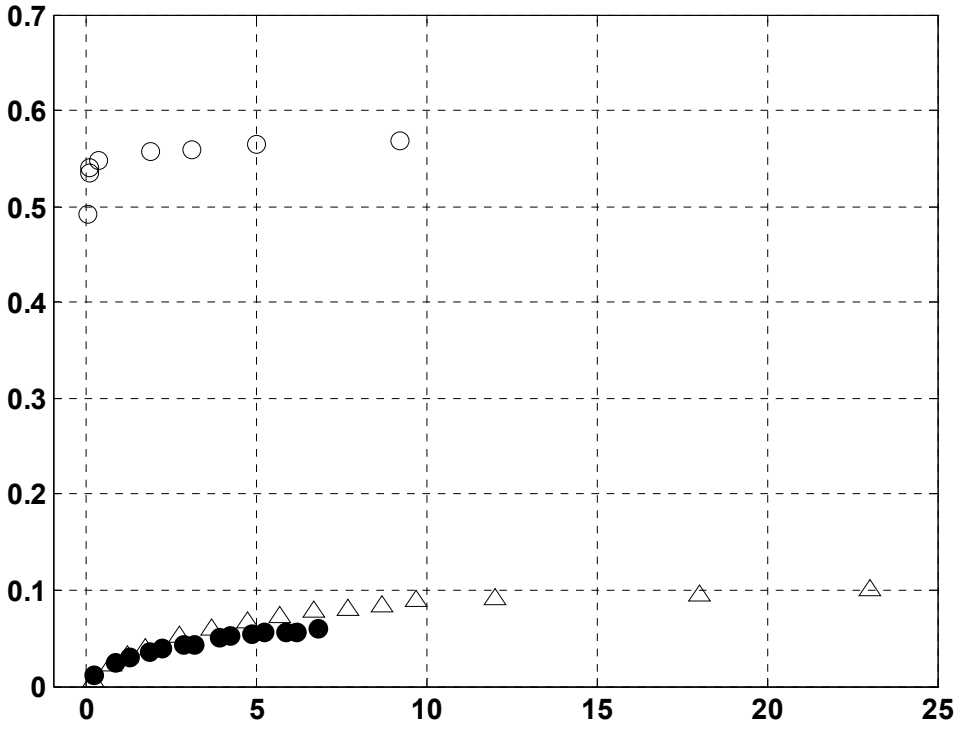

Figure 3-5: Methane excess sorption on non-powder coal cores at 13.8 MPa (•), 6.9 MPa (Δ) confining stresses and non-powder unconfined (o).

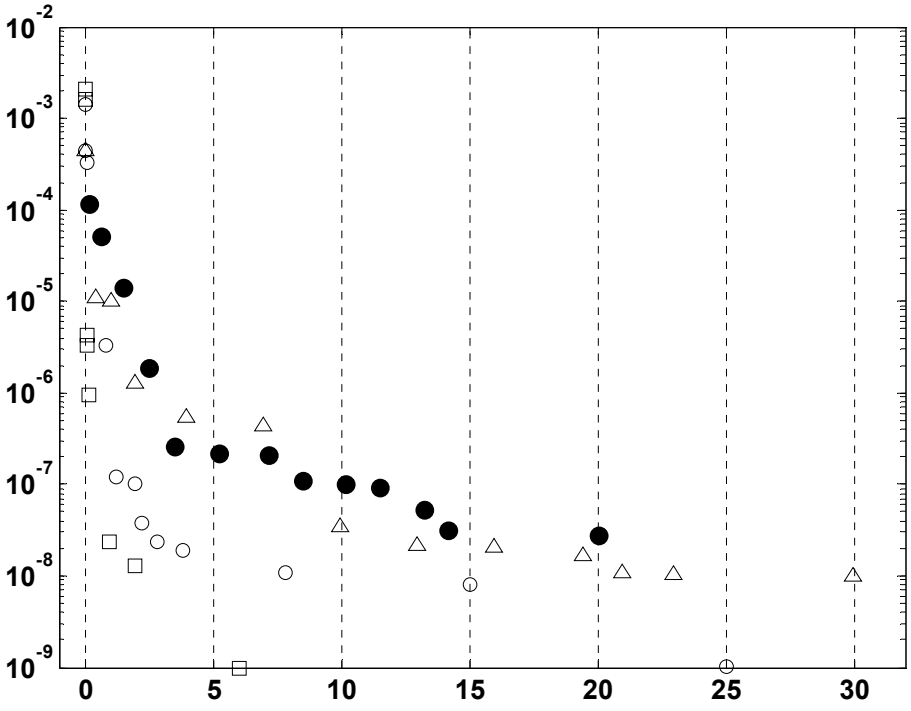

Figure 3-6: Carbon dioxide diffusivity coefficient variation as a function of time and physical state of the sample: (π) represents powder sample, (o) solid unconfined, (Δ) 6.9 MPa and (•) 13.8 MPa confining stresses.

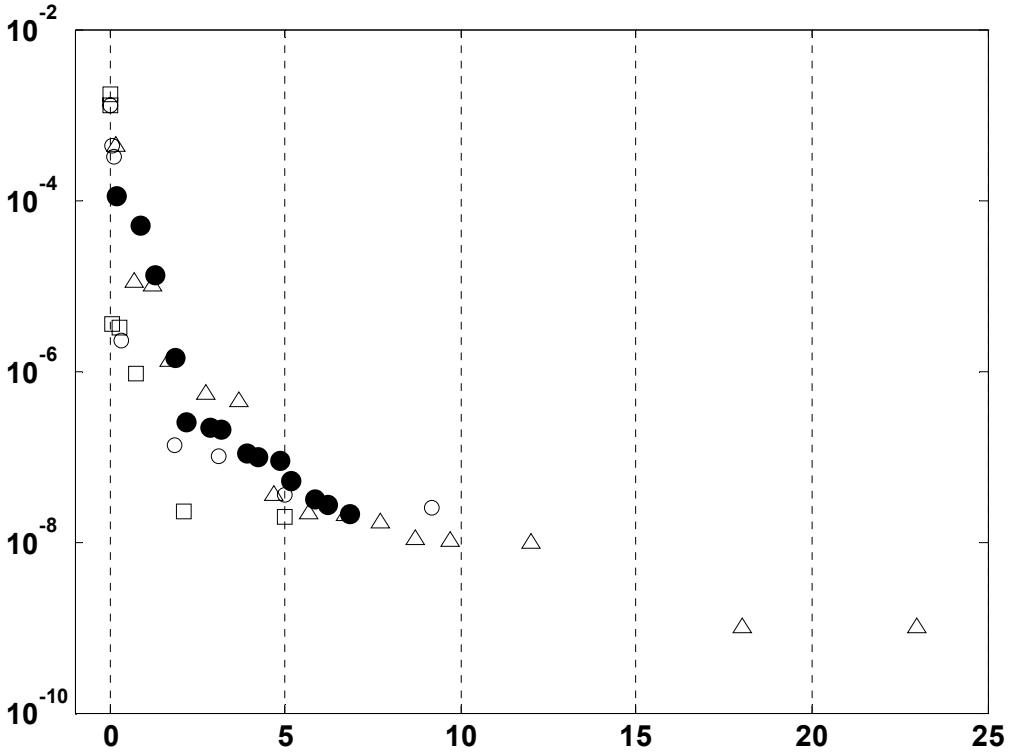

Figure 3-7: Methane diffusivity coefficient variation as a function of time and physical state of the sample: (π) represents powder sample, (o) solid unconfined, (Δ) 6.9 MPa and (•) 13.8 MPa confining stresses

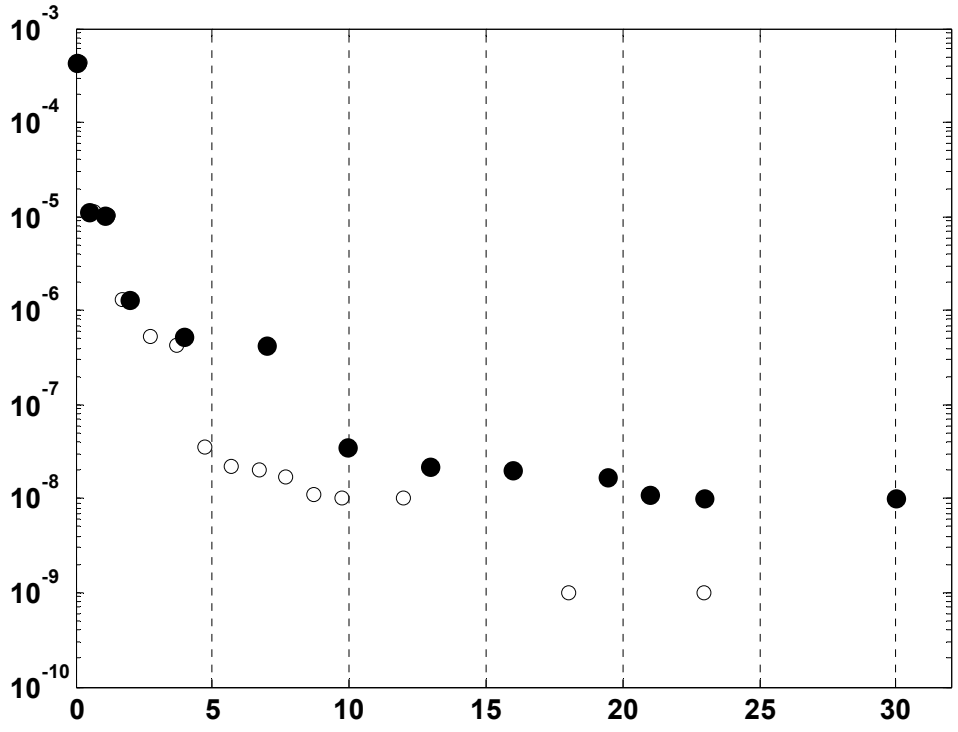

Figure 3-8: Comparison of CO_2 (•) and CH_4 (o) diffusivity coefficient variation in a 6.9 MPa confined coal core as a function of time.

Table 3-1: Proximate and ultimate coal characteristics

Proximate analysis		**Ultimate Analysis (dry basis)**		Error
Moisture	3.40	**%C**	83.05	± 0.15
Vol. Mat	37.64	**%H**	5.97	± 0.02
Fixed C	56.30	**%N**	1.44	± 0.00
Ash	2.66	**%S**	1.39	± 0.00

Table 3-2: Variation of diffusivity coefficient with time and stress state of the sample

	Initial	End	Time (days)	Cumulative uptake, mmol/g
	CO_2			
powder	2.10E-03	1.00E-09	6	1.17
solid unconfined	1.40E-03	1.01E-09	25	1.39
6.9 Mpa confining	4.36E-04	1.00E-08	30	0.85
13.8 Mpa confining	1.15E-04	2.79E-08	20	0.50
	CH_4			
powder	1.70E-03	1.92E-08	5	0.66
solid unconfined	1.25E-03	2.54E-08	9	0.57
6.9 Mpa confining	3.93E-04	1.00E-09	23	0.10
13.8 Mpa confining	1.14E-04	2.20E-08	7	0.06

Chapter 4

Dynamic Permeability of a Bituminous Coal to Carbon Dioxide Using the Transient-Pulse Method

Abstract

The need for accurate estimation of the dynamic permeability characteristics of coal seams is important considering the observed injectivity losses and its impact on the long-term sequestration operation. The injection and the subsequent interactions of coal structure with CO_2 contribute to the deformation of the coal matrix, consequently affecting the flow behavior and storage capacity. This work presents the changes in permeability of coal as a result of applied stress and CO_2 exposure time using a transient-pulse method. Coal sample permeability decreased with the increase of confining stress. Initial permeability was 0.0022 mD when subjected to 1000 psi, however, decreased around 4 times to 0.000575 mD when the confining stress was doubled. Higher confining stress reduce pore aperture, which in turn cause permeability reduction. Permeability for both confining stress values decrease over time although at different rate: 26% reduction at 1000 psi and 47 % at 2000 psi.

Introduction

Geologic sequestration of carbon dioxide into unmineable coal seam is an option for the mitigation of industrial emissions. While a solid base of knowledge and experience from oil and gas fields operations exists, data characterizing carbon dioxide movement in coal seams particularly at in-situ stress conditions is limited. The

displacement of gases in coal seam involves a complex interplay of flow in the cleat system, sorption and diffusion into the coal matrix and changes in permeability due to swelling and sorption-induced compression/compaction (Airey, 1968; Bodden III and Ehrlich, 1998; Bolt and Innes, 1959; Busch et al., 2004; Clarkson and Bustin, 1997; Gamson et al., 1993). The interactions of coal structure with injected CO_2 alter the coal matrix, consequently affecting the gas flow and storage mechanisms. The need for reliable estimation of the permeability characteristics of coal seam is dictated by considerations of the injectivity losses and its impact on the long term CO_2 sequestration or ECBM projects. Many experimental and theoretical investigations have been carried out characterizing coal gas permeability (Graham, 1919; Harpalani et al., 2006; Karlsson and Isacsson, 2003; Karn et al., 1975; Karn et al., 1970). Several factors, other than coal properties, can influence permeability. These factors include the state of stress in the sample, chemical effects, the degree of fluid saturation, and the characteristics of the permeating fluid (Ettinger et al., 1984). These conditions can change the measured permeability of a sample by several orders of magnitude (Bustin, 1997; Bustin and Clarkson, 1998).

With increasing interest in CO_2 storage and enhanced coalbed methane extraction, several theoretical models have been developed to simulate the flow of gas in coalbeds and predict long-term reservoir behavior. However, a major hindrance to the effective use of any simulator is the lack of reliable estimates of the required input parameters. Knowledge of these parameters variation is important. Such parameters include matrix deformation, sorption capacity, diffusion coefficient, and permeability. These parameters are also influenced by in-situ stress conditions, which are likely to change progressively

during injection or production, making the process of gas-flow difficult to model. Furthermore, there is a significant change in the structure of coal with CO_2 exposure, which results in a wide variation in the permeability value during the process presumably due to coal swelling (Larsen, 2004; Skawinski, 1999). To obtain information on permeability in the field is very expensive since it requires multi-well tests (Zuber and Holditch, 1996). Therefore, a laboratory method of determining changes in permeability with time is desirable. This paper presents the results of an experimental investigation to estimate the changes in permeability of coal as a result of stress and CO_2 exposure time.

Gas permeability in coal seams is one of the fundamental parameters describing the rate at which fluid moves through the structure, as well as determining the extent of effectively storing CO_2 in or extracting CH_4 from coal seam within reasonable timeframe. It is essential to simply and accurately evaluate the permeability of coal seams for efficient prediction of the long-term reservoir behavior. In general, coal is characterized as very low permeability material; therefore coal permeability cannot be effectively measured by means of standard geotechnical laboratory test methods such as the constant-head and the falling-head techniques (Zhang et al., 2000a). These later methods estimate the permeability of a saturated specimen by measuring induced flow rates under a constant or quasi-constant hydraulic gradient. However, a long time period is required to establish a steady-state flow and more importantly these flow rates are too small to monitor reliably when permeability is low. Steady-state method can only measure permeability of rocks up to 10^{-5} μm^2 (Trimmer, 1982). Furthermore, it is desirable to measure specific storage capacity routinely together with permeability rather than performing separate tests. The specific storage capacity controls the change in pore

pressure as a result of change in external pressure (Zhang et al., 2000b). Thus, if routinely performed in a systematic way, measurements of the specific storage capacity may contribute significantly to our understanding of stress transfer occurring during gas injection. The transient-pulse method permits determination of both permeability and specific storage (Hsieh et al., 1981). This technique was used in this study to investigate the permeability and specific storage of coal exposed to carbon dioxide.

Background

The concept of changes in the bulk volume of coal resulting from sorption or desorption of gas is well established. In 1932, Briggs and Sinha published a comprehensive work entitled "expansion and contraction of coal caused respectively by the sorption and discharge of gas". Briggs and Sinha (1932) demonstrated that coal swells when exposed to CO_2, that the swelling was irreversible and anisotropic with the expansion more pronounced in the direction perpendicular to the bedding plane. Many decades later, similar observations were made by different investigators (Larsen, 2004; Reucroft and Patel, 1986; Reucroft and Patel, 1983; Sethuraman and Reucroft, 1987; Walker and Mahajan, 1993). The overwhelming majority of these data, and many more available in the literature, emphasized the direct influence of coal structure changes on fundamental physical properties such as: surface area, porosity, strength, sorption capacity and permeability. Coal swelling accompanying CO_2 sorption would decrease the permeability of the coal as the volume increase is compensated within the fracture porosity (Harpalani and Chen, 1997; Harpalani and Schraufnagel, 1990). However, the

swelling may be balanced or completely neutralized by the shrinkage of the coal matrix when the uptake of gases is accompanied by desorption of CH_4 (Rogers, 1994). Thus, characterizing coal permeability is essential as it has been identified as the key parameter controlling the storage of CO_2 and the recovery of CH_4 during ECBM project (Saghafi et al., 2007). Literature on CO_2 sequestration and ECBM focuses mainly on the adsorption capacity of powder coal, the volumetric changes of the evacuated, and unconfined coal behavior at pressure-temperature conditions in the CO_2-subcritical state, while the predictability of varying permeability at in-situ conditions have received little attention. Some exceptions are available: (Harpalani and Chen, 1997) and (Cui and Bustin, 2005). The grinding introduce a more extensive system of macro-cracks, which permeates the particle and may opens up area behind closed pores (Nandi and Walker, 1970; Nandi and Walker, 1975) that may be inaccessible during CO_2 sequestration. Only when we can quantify CO_2 permeability variation in coal at simulated in-situ stress conditions, will we have the confidence to use the analytic models in reservoir simulators to predict CO_2 sequestration.

Methodology

The transient-pulse method for measuring low permeability in hydraulically tight rocks was originally introduced by Brace et al. (1968). They successfully used this technique to estimate the permeability of Westerly granite under high confining stresses. Since then, the transient-pulse technique has emerged as a reliable and established method for determining the permeability of hydraulically tight rocks (Hsieh et al., 1981;

Lin, 1978; Lin, 1982; Neuzil et al., 1981; Trimmer, 1982; Zhang et al., 2000a; Zhang et al., 2000b) and appears as appropriate method for the determination of the permeability of coal samples exposed to CO_2.

In the transient-pulse technique, the specimen is connected to two fluid reservoirs (see Fig. 4-1). By instantaneously increasing the fluid pressure in one reservoir (upstream reservoir), and measuring the corresponding pressure decay across the entire length of the specimen, the permeability can be obtained. Pressure, unlike flow-rate, does not need to be integrated over some time period and can be measured continuously in real-time with high-precision electronic transducers. This feature makes it possible to successfully conduct experiments on low-permeability specimens much faster than by using the conventional constant-head or falling-head methods.

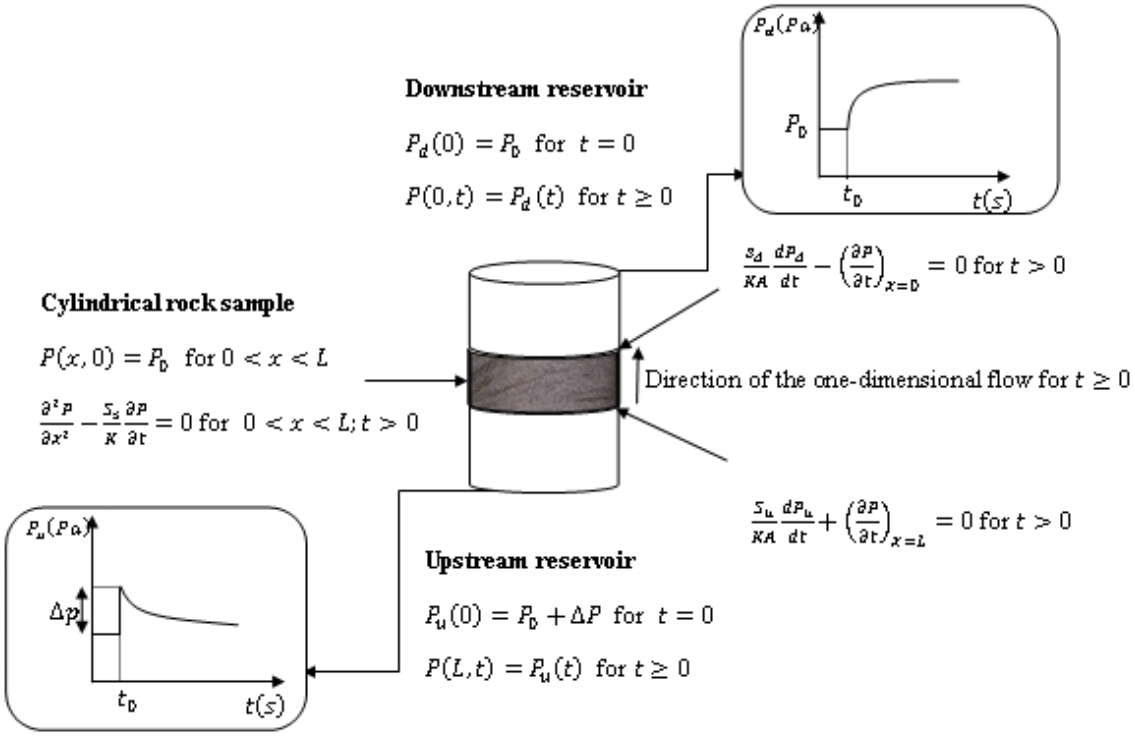

Figure 4-1: Schematic representation of transient-pulse method with boundaries conditions

The exact solution to the transient-pulse permeability test derived by Hsieh et al. (1981) and the companion graphical method proposed by Neuzil et al. (1981) allow both the permeability and the specific storage of a specimen to be determined. However, the attendant procedures are relatively complicated and many investigators prefer the solution proposed by Brace et al. (1968) to interpret their experimental results. Thus, only an estimate of permeability is obtained and specific storage capacity is neglected. However, the specific storage capacity is an equally important hydraulic property associated with transient-flow processes in porous media. The representative permeability of a specimen measured in the laboratory should be obtained under environmental

conditions that closely simulate those found in situ, notably confining and pore pressures, the temperature, and the hydraulic gradient. In this study, the specific storage capacity and the permeability variation on coal specimen under stresses were quantified. An exact solution of the transient-pulse technique as presented by Hsieh et al. (1981) was applied.

Transient-Pulse Mathematical Formulation

A schematic representation illustrating the initial and boundary conditions for the transient pulse permeability test is depicted in Figure 4-1 (Brace et al., 1968; Hsieh et al., 1981).

Initially, the sample is saturated and the fluid pressure inside the sample and the reservoirs is uniform (P_0).

$$P(x, t = 0) = P_0 \text{ for } 0 < x < L \quad (1)$$

With $x(m)$, the distance along the sample, $P(Pa)$ the pore pressure in the sample and $P_0(Pa)$ the initial pore pressure in the sample.

An increment of pressure, ΔP, is carried out in the upstream reservoir (equation 2). The pressure in the upstream and the downstream reservoirs are respectively defined as P_u (equation 4) and P_d (equation 5).

$$P_u(0) = P_0 + \Delta P \quad \text{for} \quad t = 0 \quad (2)$$

$$P_d(0) = P_0 \quad (3)$$

$$P(L, t) = P_u(t) \quad \text{for} \quad t \geq 0 \quad (4)$$

$$P(0, t) = P_d(t) \quad \text{for} \quad t \geq 0 \quad (5)$$

This pulse creates a one-dimensional flow through saturated porous sample (equation 6), which combines the principle of conservation of fluid mass in a deformable matrix and Darcy's law for laminar flow through a hydraulically isotopic matrix.

$$\frac{\partial^2 P}{\partial x^2} - \frac{S_s}{K}\frac{\partial P}{\partial t} = 0 \quad \text{for } 0 < x < L \text{ and } t > 0 \tag{6}$$

Where t is time (s), S_s is specific storage capacity of the sample and is expressed as $\gamma_w \varphi C_w$ (γ_w is the specific gravity of the permeating fluid, φ the sample porosity and C_w the compressibility (Pa^{-1})) and K is expressed as $k\gamma_w/\eta$ (k is the permeability (m^2) and η the viscosity $(Pa\ s)$). In addition, the fluid mass conservation at the sample/reservoir interfaces is translated into the boundary conditions (equation 7) and (equation 8).

$$\frac{S_d}{KA}\frac{dP_d}{dt} - \left(\frac{\partial P}{\partial x}\right)_{x=0} = 0 \text{ for } t > 0 \tag{7}$$

$$\frac{S_u}{KA}\frac{dP_u}{dt} + \left(\frac{\partial P}{\partial x}\right)_{x=L} = 0 \text{ for } t > 0 \tag{8}$$

Where S_d and $S_u(m^2)$ are the compressive storage of the downstream and upstream reservoirs; A is the cross sectional area of the sample perpendicular to the flow direction (m^2). Hsieh et al. (1981) solved this initial-boundary value problem defined by the Eqs. (1)-(8), by the Laplace transform method. They offered a general analytical solution with dimensionless variables and parameters. The solution for the pressure evolution in the upstream and downstream reservoirs is given by Eqs. (9) and (10).

$$\frac{P_u(t)-P_0}{\Delta P} = \frac{1}{1+\beta+\gamma} + 2\sum_{m=1}^{\infty} \frac{(\beta+\gamma^2\emptyset_m^2/\beta)\exp(-\alpha\emptyset_m^2 t)}{\gamma^2\emptyset_m^2/\beta^2+(\gamma^2\beta+\gamma^2+\gamma+\beta)\emptyset_m^2/\beta+(\beta^2+\gamma\beta+\beta)} \tag{9}$$

$$\frac{P_d(t)-P_0}{\Delta P} = \frac{1}{1+\beta+\gamma} + 2\sum_{m=1}^{\infty} \frac{(\beta-\gamma\emptyset_m^2/\beta)\exp(-\alpha\emptyset_m^2 t)}{\gamma^2\emptyset_m^2/\beta^2+(\gamma^2\beta+\gamma^2+\gamma+\beta)\emptyset_m^2/\beta+(\beta^2+\gamma\beta+\beta)\cos\emptyset_m} \tag{10}$$

Where $\emptyset_m\,(m = 1, 2, \ldots, \infty)$ is the positive root of the following equation which can be obtained by Newton's method:

$$\tan \emptyset_m = \frac{(\gamma+1)\emptyset_m}{\gamma\emptyset_m^2/\beta+\beta} \tag{11}$$

And α, β and γ are defined by the following equations:

$$\alpha = \frac{K}{L^2 S_s} \tag{12}$$

$$\beta = \frac{S_s AL}{S_u} \tag{13}$$

$$\gamma = \frac{S_d}{S_u} \tag{14}$$

In comparison with equation (9) and equation (10), the mathematical analysis developed by Brace et al. (1968) for the transient pulse permeability test assumes that there is no compressive storage in the sample, in which case the second term in (6) vanishes, and the solution for the pressure decay at the upstream reservoir is exponential. Brace et al. (1968) studied a crystalline rock (granite), which generally have small porosity and little compressive storage. Neuzil et al. (1981) stated that the application of this approach for permeability determination of rocks with significant porosity and large compressive storage was incorrect. The specific storage capacity, S_s, is a function of the compressibility of the pore fluid, the bulk and matrix compressibility, and the interconnected porosity of the specimen (Zhang et al., 2000b). Consequently, the specific storage capcity is equally an important property for characterizing transient flow in coal and other structure with significant porosity.

Experimental Procedure

Sample Preparation

The coal sample used for this study was prepared from a single block collected from the Hazard No. 9 coal seam, Perry County of the Western Kentucky Coalfield. The highwall overburden, mostly sandstone was estimated to be 200 m thick and the seam to be 2 m thick. The block was removed and coated with water-based polycrylic protective finish to prevent any further oxidation and dehydration of the sample. It was cast in plaster to aid coring process. The core was preserved in sealed container under nitrogen environment. The end surfaces of the core were polished to produce a flat and parallel surface for the application of uniform stress and gas distribution. A core sample of 2.5 cm (1 inch) in diameter and 1.8 cm (0.7 inch) length was hydraulically confined to replicate the in-situ stress conditions during flow experiments.

Permeability Measurements

Permeability and specific storage capacity were extracted from pressure-decay data in the upstream reservoir. A Microsoft Excel® solver was developed to simultaneously obtained permeability and specific storage capacity by minimizing the sum of square errors between the theoretical values from equation 9 and the experimental data. The upstream reservoir, downstream reservoir and the coal sample were initially equilibrated at 450 psi gas pressure. A transient-pulse of 45 psi representing 10% of the

downstream pressure was then injected. The upstream and downstream pressures were recorded with high-precision pressure transducers at 2 seconds intervals. Equilibrium time after the pulse varies from few minutes to hours, depending on the stress conditions. After equilibrium, the system was allowed to bleed gas at very slow rate till the initial pressure value was reached. Twenty-four hours was allowed before the next pulse. The process was repeated for 10 days. Confining stresses of 1000 psi and 2000 psi corresponding to an equivalent depth of 1000 and 2000 feet were employed. Values of the physical constants for the calculations were obtained from Fischer and Paterson (1992) and Span and Wagner (1996). The upstream and downstream reservoirs capacities were respectively 54.15 ml and 41.68 ml.

Results and Discussion

To evaluate the influence of confining stress on permeability of a coal sample, experiments were conducted with constant CO_2 pressure of 450 psi. For each specific value of confining stress, permeability was measured at 24 hours interval repeated over several days to assess the impact of exposure time on the coal matrix permeability. Figure 4-2 is a sample representation of the upstream and downstream pressures variation. The influence of confining stresses on pressure variation is depicted on Figure 4-3. An example of dynamic curve fitting for the determination of permeability and specific storage capacity is presented on Figure 4-4. Permeability measurements for 1000 and 2000 psi confining stress values, simulating an approximate depth of 1000 and 2000 feet are shown in Figure 4-5.

Results presented on Figure 4-4 and 4-5 emphasized that permeability decreased with the increase in confining stress. The permeability of rocks is related to the degree of stress to which they are subjected (Brighenti, 1989). The confining stress reduce pores aperture, which causes the decrease in permeability. Similar variation of coal permeability with increasing confining stress has been demonstrated for a variety of stress magnitudes (Enerver et al., 1994). A theoretical relationship between coalbed permeability and stress was developed by McKee et al. (1987) that showed permeability declining exponentially with increasing stress. However, although, the permeability reduction of confining sample has been mostly attributed to the confining stress, there are endogenous factors which influence coal permeability variation. Bustin (1997) measured the permeability of coal seam core samples that were subjected to varying levels of effective stress and found that there was no direct relationship between effective stress and permeability. Permeability was clearly a function of effective stress, but the coal seam composition and degree of fracturing also appeared to be controlling factors. The highest permeability was found in coal samples with at least one well-developed fracture set and such samples were usually rich in vitrinite. Samples with the lowest permeability were typically low in vitrinite and contained significant mineralization. Consequently, although an overall decreasing trend exist between increasing confining stress and permeability reduction, the sensitivity of permeability to coal macerals, degree of fracturing and mineralization emphasized that accurate interpretation of coal permeability variation required consideration of coal physical, chemical and optical characteristics.

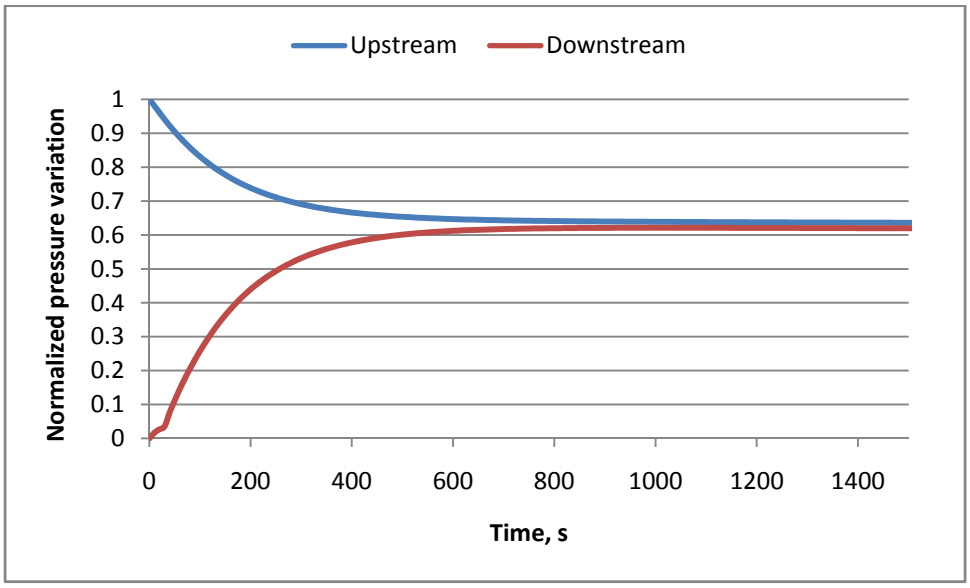

Figure 4-2: Upstream and downstream pressures variation during the transient-pulse.

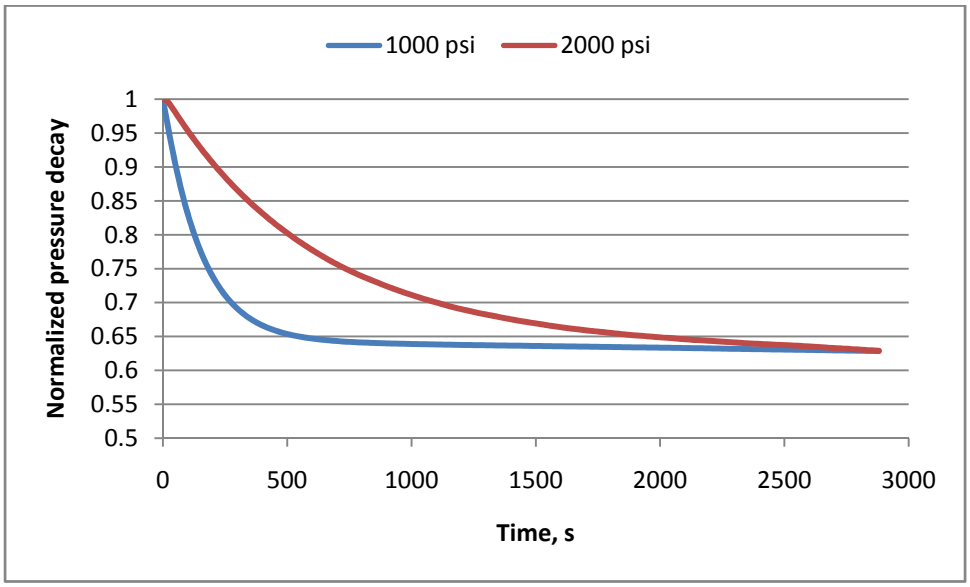

Figure 4-3: Influence of confining stress on upstream reservoir pressure decay.

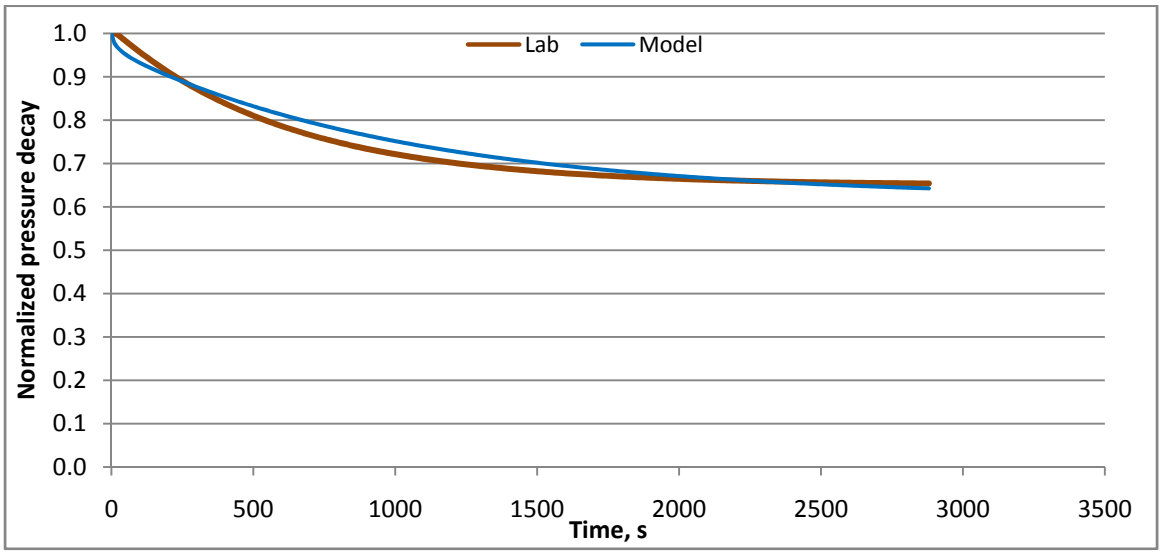

Figure 4-4: Curve fitting for the determination of permeability and specific storage capacity

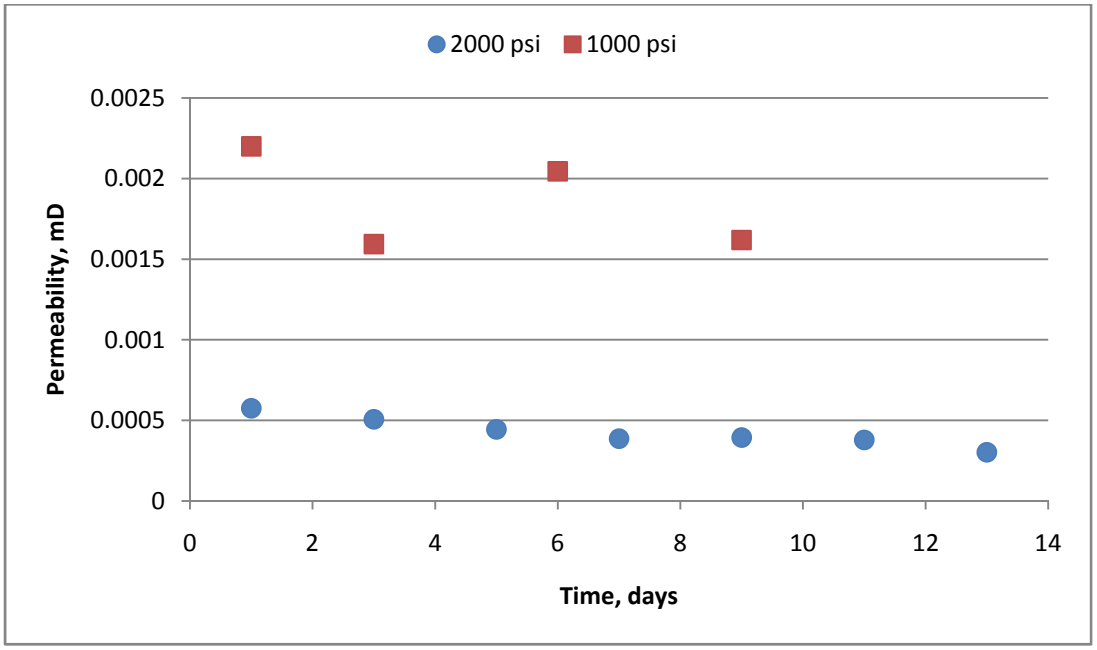

Figure 4-5: Permeability variation as a function of time of a bituminous coal at 1000 and 2000 psi confining stress

Permeability obtained varied only between 0.0022 mD (milidarcy) and 0.001619 mD for 1000 psi and 0.000575 to 0.000302 mD for 2000 psi confining stress. Such low permeabilities raise concerns on the practicality of carbon dioxide storage in coal seams. In-situ permeability is, however expected to be several orders of magnitude greater. Bustin (1997) attributes this discrepancy to the greater fracture interconnectivity experienced by rocks in the subsurface as compared to test samples. The difference between laboratory and field permeabilities could also be attributed to fractures that form a partly open, interconnected, three-dimensional system within the reservoir rocks through which fluid flows preferentially in certain directions (Grout, 1991). Finally, the use of hydrostatic or triaxial stress regimes during experimentation, whereas in-situ coals are subjected to a uniaxial stress may also play a role.

Permeability of the coal sample obtained at constant injection gas pressure and confining stress at 24 hours interval during about 10 days showed a slight decrease of permeability over time. While the initial permeability is different for each confining stress, results indicated that the permeability is influenced with CO_2 exposure time. Permeability reduction was 26 % and 47% for both 1000 and 2000 psi confining stress respectively.

Under these confining stress conditions the specific storage capacity was determined to be $2.33\ x\ 10^{-5}m^{-1}$ and did not decrease with the increase of hydrostatic loading or time.

Conclusions

Experimental method is of fundamental importance to reliably characterize the sensitivity of permeability variation of coal sample during gas injection. Results show that the transient-pulse methods can be used effectively to determine the permeability of confined coal. Coal sample permeability decreased with the increase of confining stress. Average permeability was 0.001865 millidarcies (mD) when subjected to 1000 psi (6.9 MPa) and decrease around 4 times to 0.000427 millidarcies (mD) when the confining stress was doubled. Higher confining stress close reduce pore aperture, which in turn cause permeability reduction. Permeability for both confining stress values decrease over time although at different rate: 26% reduction at 1000 psi and 47 % at 2000 psi (13.8 MPa). This reduction can be attributed to coal compression/compaction phenomenon when exposed to CO_2. Specific storage coefficient was determined to be $2.33\ x\ 10^{-5}m^{-1}$ and did not decrease with the increase of confining stress and time. This indicated that the time required for the pulse was not enough to induce any stress transfers in the coal matrix.

References

Airey, E.M., 1968. Gas emission from broken coal . An experimental and theoretical investigation. International Journal of Rock Mechanics and Mining Sciences, 5(6): 475.

Bodden III, W.R. and Ehrlich, R., 1998. Permeability of coals and characteristics of desorption tests: Implications for coalbed methane production. International Journal of Coal Geology, 35(1-4): 333-347.

Bolt, B.A. and Innes, J.A., 1959. Diffusion of carbon dioxide from coal. Fuel, 38(3): 333-337.

Brace, W.F., Walsh, J.B. and Frangos, W.T., 1968. Permeability of granite under high pressure. Journal of Geophysical Research, 73(6): 2225-2236.

Briggs, H. and Sinha, R.P., 1932. Expansion and contraction of coal caused respectively by sorption and discharge of gas. Proceedings of the Royal Society of Edinburgh, 53(1): 48-53.

Brighenti, G., 1989. Effect of confining pressure on gas permeability of tight sandstones. In: V. Maury and D. Fourmaintraux (Editors), Rock at Great Depth. Balkema, Rotterdam, pp. 187-194.

Busch, A., Gensterblum, Y., Krooss, B.M. and Littke, R., 2004. Methane and carbon dioxide adsorption-diffusion experiments on coal: upscaling and modeling. International Journal of Coal Geology, 60(2-4): 151-168.

Bustin, R.M., 1997. Importance of fabric and composition on the stress sensitivity of permeability in some coals, Northern Sydney Basin, Australia: relevance to coal bed methane exploitation. American Association of Petroleum Geologists Bulletin, 81(11): 1894 -1908.

Bustin, R.M. and Clarkson, C.R., 1998. Geological controls on coalbed methane reservoir capacity and gas content. International Journal of Coal Geology, 38(1-2): 3-26.

Clarkson, C.R. and Bustin, R.M., 1997. Variation in permeability with lithotype and maceral composition of Cretaceous coals of the Canadian Cordillera. International Journal of Coal Geology, 33(2): 135-151.

Cui, X. and Bustin, R.M., 2005. Volumetric strain associated with methane desorption and its impact on coalbed gas production from deep coal seams. American Association of Petroleum Geologists Bulletin, 89(9): 1181-1202.

Enerver, J.R., Pattison, C.I., McWatters, R.J. and Clark, I.H., 1994. The relationship between in-situ stress and reservoir permeability as a component in developing an exploration strategy for coalbed methane in Australia., EUROCK '94, SPE-ISRM Rock Mechanics in Petroleum Engineering. Balkema, Rotterdam, pp. 163 - 171.

Ettinger, I.L., Lidin, G.D., Shulman, N.V., Kovaleva, I.B. and Radchenko, S.A., 1984. Coal seam temperature-variation as an indicator of mechanical and physicochemical processes in the seam. Soviet Mining Science USSR, 20(5): 395-398.

Fisher, G.J. and Paterson, M.S., 1992. Measurement of permeability and storage capacity in rocks during deformation at high temperature and pressure. In: B. Evans and T. Wong (Editors), Fault Mechanics and Transport Properties of Rocks. Academic Press, London, pp. 213-252.

Gamson, P.D., Beamish, B.B. and Johnson, D.P., 1993. Coal microstructure and micropermeability and their effects on natural gas recovery. Fuel, 72(1): 87-99.

Graham, I.J., 1919. The permeability of coal to gases. Transaction of the Institution of the Mining Engineers, 58(1): 32-38.

Grout, M.A., 1991. Cleats in coalbed of Southern Piceane Basin, Colorado - Correlation with regional and local fracture sets in associated clastic rocks. In: S.D. Schwochow, D.K. Murray and M.F. Fahy (Editors), Coalbed methane of Western North America. Rocky Mountain Association of Geologists, Denver, pp. 35-49.

Harpalani, S. and Chen, G., 1997. Influence of gas production induced volumetric strain on permeability of coal. Geotechnical and Geological Engineering, 15(4): 303-325.

Harpalani, S., Prusty, B.K. and Dutta, P., 2006. Methane/CO_2 sorption modeling for coalbed methane production and CO_2 Sequestration. Energy & Fuels, 20(4): 1591-1599.

Harpalani, S. and Schraufnagel, R.A., 1990. Shrinkage of coal matrix with release of gas and its impact on permeability of coal. Fuel, 69(5): 551-556.

Hsieh, P.A., Tracy, J.V., Neuzil, C.E., Bredehoeft, J.D. and Silliman, S.E., 1981. A transient laboratory method for determining the hydraulic-properties of tight rocks .1. Theory. International Journal of Rock Mechanics and Mining Sciences, 18(3): 245-252.

Karlsson, R. and Isacsson, U., 2003. Laboratory studies of diffusion in bitumen using markers. Journal of Materials Science, 38(13): 2835-2844.

Karn, F.S., Friedel, R.A. and Sharkey, J.A.G., 1975. Mechanism of gas flow through coal. Fuel, 54(4): 279-282.

Karn, F.S., Friedel, R.A., Thames, B.M. and Sharkey, J.A.G., 1970. Gas transport through sections of solid coal. Fuel, 49(3): 249-256.

Larsen, J.W., 2004. The effects of dissolved CO_2 on coal structure and properties. International Journal of Coal Geology, 57(1): 63-70.

Lin, W., 1978. Determination of rock permeability using transient method. Transactions-American Geophysical Union, 59(12): 1193-1193.

Lin, W., 1982. Parametric analyses of the transient method of measuring permeability. Journal of Geophysical Research, 87(Nb2): 1055-1060.

McKee, C.R., Bumb, A.C. and Koenig, R.A., 1987. Stress-dependent permeability and porosity of coal, Coalbed Methane Symposium, Tuscaloosa, AL, pp. paper 8742.

Nandi, S.P. and Walker, J.P.L., 1970. Activated diffusion of methane in coal. Fuel, 49(3): 309-323.

Nandi, S.P. and Walker, J.P.L., 1975. Activated diffusion of methane from coals at elevated pressures. Fuel, 54(2): 81-86.

Neuzil, C.E., Cooley, C., Silliman, S.E., Bredehoeft, J.D. and Hsieh, P.A., 1981. A transient laboratory method for determining the hydraulic-properties of tight rocks .2. Application. International Journal of Rock Mechanics and Mining Sciences, 18(3): 253-258.

Reucroft, P.J. and Patel, H., 1986. Gas-induced swelling in coal. Fuel, 65(6): 816-820.

Reucroft, P.J. and Patel, K.B., 1983. Surface area and swellability of coal. Fuel, 62(3): 279-284.

Rogers, R.E., 1994. Coalbed Methane Principles and Practice. P T R Prentice Hall, NJ 07632, 339 pp.

Saghafi, A., Faiz, M. and Roberts, D., 2007. CO_2 storage and gas diffusivity properties of coals from Sydney Basin, Australia. International Journal of Coal Geology, 70(1-3): 240-254.

Sethuraman, A.R. and Reucroft, P.J., 1987. Gas and vapor induced coal swelling, Prepr. Pap. Am. Chem. Soc., Div. Fuel Chem., Denver, CO, USA, pp. 259-264.

Skawinski, R., 1999 Considerations referring to coal swelling accompanying the sorption of gases and water. Arch. Min. Sci., 44: 425-434.

Span, R. and Wagner, W., 1996. A new equation of state for carbon dioxide covering the fluid region from the triple-point temperature to 1100 K at pressures up to 800 MPa. Journal of Physical and Chemical Reference Data, 25: 1509-1596.

Trimmer, D., 1982. Laboratory measurements of ultralow permeability of geologic materials. Review of Scientific Instruments, 53(8): 1246-1254.

Walker, P.L. and Mahajan, O.P., 1993. Pore structure in coals. Energy & Fuels, 7(4): 559-560.

Zhang, M., Takahashi, M., Morin, R.H. and Esaki, T., 2000a. Evaluation and application of the transient-pulse technique for determining the hydraulic properties of low-permeability rocks - Part 1: Theoretical evaluation. Geotechnical Testing Journal, 23(1): 83-90.

Zhang, M., Takahashi, M., Morin, R.H. and Esaki, T., 2000b. Evaluation and application of the transient-pulse technique for determining the hydraulic properties of low-permeability rocks - Part 2: Experimental application. Geotechnical Testing Journal, 23(1): 91-99.

Chapter 5

Summary and Conclusions

The hypothesis of this thesis was that the extent of deformation determines the dynamic permeability and hence the transport of gas in coal, influencing both the rate and capacity of the coalbed to accommodate CO_2 storage and provide methane production. An experimental investigation characterizing the three-dimensional regional coal matrix deformation upon carbon dioxide sorption, desorption and the application of confining stresses with evacuated bituminous coal cores was conducted. Methane and carbon dioxide sorption capacities and sorption rates on powdered, non-powdered unconfined and non-powdered confined cores were evaluated. The dynamic permeability of a coal sample under in-situ stress conditions was determined. Bituminous coal samples used were prepared from a single block collected from the Hazard No. 9 coal seam, Perry County of the Western Kentucky Coalfield. The following conclusions and observations were made:

1. Deformations of coal upon stress application, CO_2 sorption or desorption are highly heterogeneous and lithotypes dependent. Alternating positive and negative strain values observed at different locations during compression, sorption and desorption emphasized that compression/compaction and expansion of coal occurs during CO_2 sequestration. Swelling of coal during CO_2 sorption was not balance by the shrinkage after the release of CO_2 to atmospheric pressure. Coal swelled even under the confining stress applied here although to limited

extent. This implies that the application of geodesy techniques or tiltmeters for CO_2 verification and monitoring may be limited due to minor swelling.

2. The sorption capacity and the diffusion of gas in coal are both influenced by the stress state of the sample. The application of confining stress contributed to both CH_4 and CO_2 sorption capacity reduction. Due to presumed CH_4 limited ability to dissolve in coal matrix compared to CO_2, its sorption capacity reduction was more pronounced. The diffusion of CH_4 and CO_2 in confined coal is described with varying diffusivity coefficients throughout the sorption process. It is evident that CH_4 and CO_2 sorption and transport in coal should be characterized differently, specifically when dealing with non-powder confined samples. Consequently, although powdered coal samples provide a quick indication of the sorption capacity, it does not capture the dynamics of interrelated processes occurring at in-situ stress conditions and is not applicable for geological sequestration estimates.

3. The transient-pulse methods can be used effectively to determine the permeability of confined coal rapidly. Coal permeability varies widely and decreases with increasing confining stress, likely as a result of cleats and pores aperture reduction with increasing effective stress. Coal permeability also decreases over time even at constant effective stress. This reduction can be attributed to coal swelling, structure

rearrangement and compression/compaction phenomenon when exposed to CO_2.

Coal is a complex and heterogeneous structure composed of macerals and minerals occurring in distinct associations called lithotypes. Each lithotype has a set of physical and chemical characteristics which affect the overall gas sorption and flow behavior. In addition to compositional factors, coal properties also change with the degree of coalification. The difference in sorption and flow behavior observed from the coal samples at different physical state of stress can best be explained in terms of macropore, micropore and matrix components of the coal. These components are affected differently by the confining stress and the subsequent deformation induced by exposure to gas. Equally significant, it also suggests that the connectivity of coal's microstructures, the continuity of pores network that is influenced by the degree of fractures mineralization will play a significant role on the overall gas sorption, and are likely to contribute significantly to the flow of gas through coal during sequestration or methane production. No accounting for decreasing CO_2 storage potential and permeability reduction at increasing depth, temperature, moisture content and at the presence of methane and other gases existing in unmineable coal seams are erroneous although some of these factors may be mitigated through storage efficiency factor. Thus, it seems likely that the nature of the reduction observed in this thesis may be captured via these efficiencies, without explicitly recognizing the influence of stress. Either way, future work should focus on these issues and in better quantifying the capacity of whole coals under stress, and the interplay of the competing processes to enable meaningful predictions. Considering the heterogeneity and the variability of coal behavior as stated,

the generalization of these results should be done cautiously, because the above mentioned differences have important implications for gas storage or production from coal. Improved representation of the physical state of coal is needed to better characterize, quantify and confidently utilize unmineable coal seams as storage for CO_2. Data characterizing sorption and diffusion of gases in coal at in-situ conditions are limited and it is required to investigate this behavior further. Current capacity estimates for CO_2 sequestration in coal are uncertain because of lack of field experience, experiments at in situ conditions and due to the challenges of the scientific approach with such a variant material and complex set of competing processes. Future research for CO_2 sequestration in coal is essential and should aim toward in-situ sorption and dissolution rates of injected CO_2, competitive sorption, structure rearrangement and the resulting rate of change in permeability. Only through further scientific investigation of these in-situ effects can we confidently determine the viability of coal seams reservoirs.

VITA

Denis Pone

EDUCATION

Ph.D. Energy and Geo-Environmental Engineering, Penn State University, U.S.A.	*2006-2009*
M.S. Geosciences , University of the Witwatersrand, Johannesburg , South Africa	*2004-2005*
M.S. Physics , University of Douala, Cameroon	*2001-2003*
B.S. Physics, University of Douala, Cameroon	*1997-2001*

PROFESIONAL CERTIFICATION

Sustainable Development in Mining, University of the Witwatersrand	*2005*

AWARDS

SPE- Mid-Continent/Rocky Mountain/Eastern Regional Student Contest Award, 1st Place	*2008*
Outstanding Teaching Assistant for General Education, Penn State University	*2008*
Medlin Scholarship Award in Coal Geology, Geological Society of America	*2007*
Charles B. Darrow Award in Coal Utilization, Penn State University	*2007*
Two months research fellowship at USGS, Reston, VA. May and June, 2005	*2005*
Postgraduate Merit Awards, University of the Witwatersrand	*2005*
Bradlow Merit Awards, University of the Witwatersrand	*2005*

PUBLICATIONS

Pone, J. D. N., M. Hile, P. M. Halleck, J. P. Mathews, 2009. Three-dimensional carbon dioxide-induced strain distribution within a confined bituminous coal. International Journal of Coal Geology*,* 77(1-2)103-108

Pone, J. D. N., P. M. Halleck, J. P. Mathews, 2008. Characterization of coal for sequestration and enhanced coalbed methane recovery at in situ conditions. Asia Pacific Coalbed Methane Symposium, Brisbane, Australia, September 22-24, 2008.

Pone, J. D. N., P. M. Halleck, J. P. Mathews, 2008. Methane and carbon dioxide sorption and transport rate in coal at in-situ conditions. The 9th International Conference on Greenhouse Gas Technologies, 16 – 20 November, 2008, Washington DC, USA

Pone, J. D. N., Hein, K. A. A.; Stracher, G. B.; Annegarn, H. J.; Finkleman, R. B.; Blake, D. R.; McCormack, J. K.; Schroeder, P., The spontaneous combustion of coal and its by-products in the Witbank and Sasolburg coalfields of South Africa. International Journal of Coal Geology , 2007, 72, 124-140

Pone, J.D.N., Hein, K.A.A., Annegarn, H.J., Stracher, G.B., Finkelman, R.B., 2007. Spontaneous combustion of coal: gases and solids mobilized. International Pittsburgh Coal Conference 2007, Johannesburg, South Africa. September 10-14, 2007

Pone, J. D. N., Hein, K. A. A.; Stracher, G. B.; Annegarn, H. J.; Finkleman, R. B.; Potential health and environmental impacts of burning coal in the Witbank coalfield of South Africa. **ERSEC/UNESCO** Ecological **Book Series – 4** on Coal Fire Research*,* 2008.

Pone, J.D.N., Stracher, G.B., Finkelman, R.B., Annegarn, H.J., Hein, K.A.A., 2005. Environmental impacts of coal fires: Spontaneous combustion in South Africa. ERSEC Conference Programs and Abstracts, p 94-95

Stracher, G.B., Tabet, D.E., Anderson P.B., **Pone, J.D.N**., 2005. Utah's State rock and the Emery Coalfield. Geology, mining, and natural burning coal beds. The Geological Society of American Field Guide.

Stracher, G.B., **Pone, J.D.N**., 2005. Finkelman, R.B., McCormack, J., Annegarn, H.J., and Blake, D. Gas vent mineralization: spontaneous combustion by-products of South African coal mine fires. Geological Society of American Programs and Abstracts.